# Supporting Information

## A modular probe strategy for drug localization, target identification and target occupancy measurement on single cell level

Anna Rutkowska[1], Douglas W. Thomson[1], Johanna Vappiani, Thilo Werner, Katrin Mueller, Lars Dittus, Jana Krause, Marcel Muelbaier, Giovanna Bergamini[2*] and Marcus Bantscheff[2*]

Cellzome GmbH, a GlaxoSmithKline company, Meyerhofstrasse 1, D- 69117 Heidelberg, Germany

1) 2) these authors contributed equally
*) Authors for correspondence: Giovanna.2.Bergamini@GSK.com; Marcus.x.Bantscheff@GSK.com

**Contents**

## Figure S1

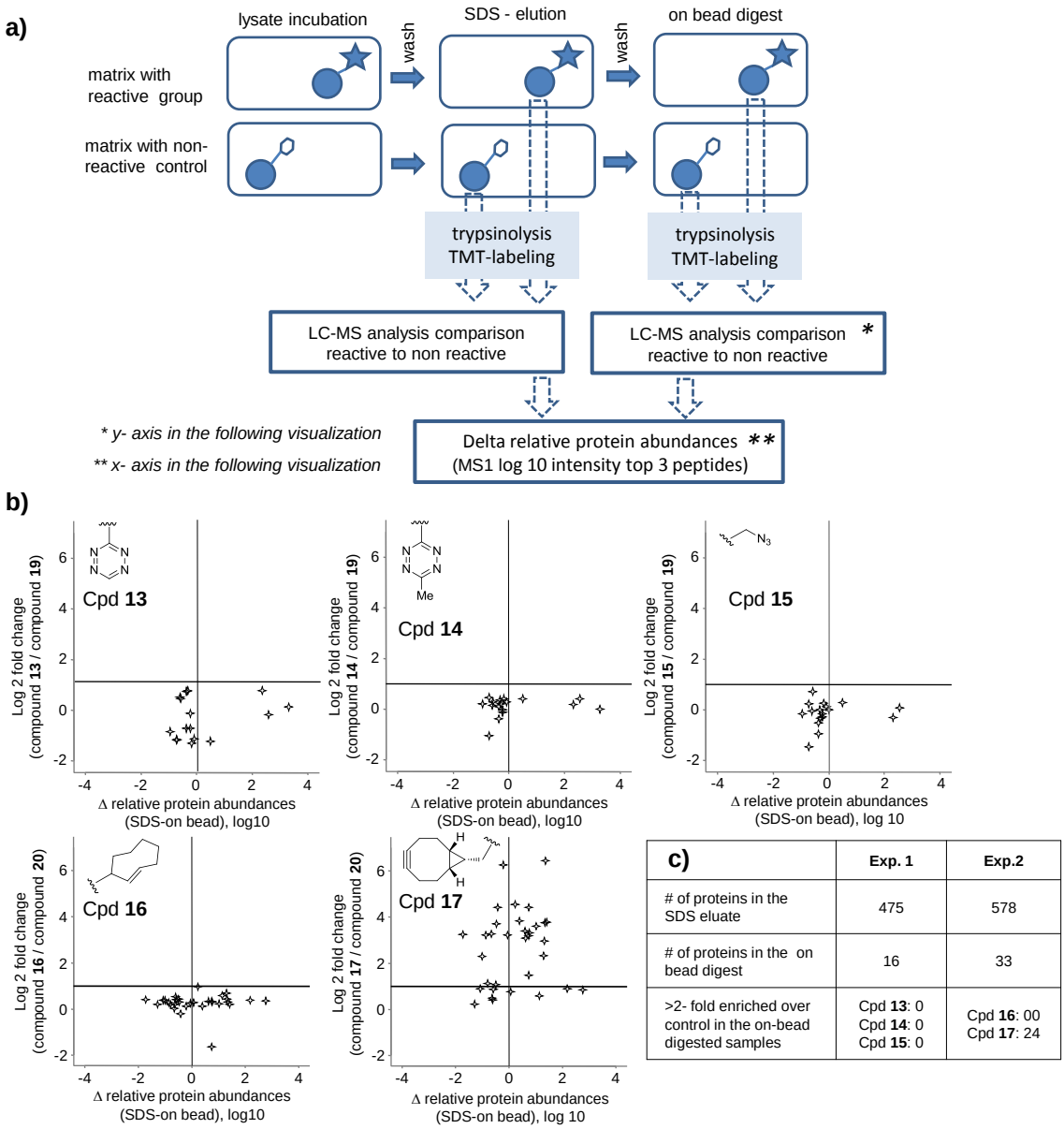


| c) | Exp. 1 | Exp.2 |
|---|---|---|
| # of proteins in the SDS eluate | 475 | 578 |
| # of proteins in the on bead digest | 16 | 33 |
| >2- fold enriched over control in the on-bead digested samples | Cpd **13**: 0<br>Cpd **14**: 0<br>Cpd **15**: 0 | Cpd **16**: 00<br>Cpd **17**: 24 |

**Figure S1.** a) **A schematic representation of the experiment design to assess reactivity of bioorthogonal moieties with proteins**. Compounds **13, 14, 15** containing the bioorthogonal moieties tetrazine, methyl-tetrazine, azide and the unreactive control compound **19** were each immobilized on streptavidin beads and incubated with K-562 cell lysates. The proteins captured via a non-covalent mechanism were eluted with SDS followed by trypsin digestion. Subsequently, proteins that were bound covalently were trypsinized directly on the streptavidin beads. Tryptic peptides were then encoded with isobaric mass tags enabling quantification of protein abundances in each sample relative to the unreactive control. In a separate experiment protein binding of compounds **16** and **17** containing the TCO* and BCN groups was compared to the unreactive control compound **20**. b) **A graphical representation of the observed reactivity**. On the x-axis protein abundances as estimated from MS1 signal intensities (TOP3 method) are compared between SDS eluates and on-bead digested samples. Notably, all proteins observed in the on-bead digested samples were also identified with SDS elution and only proteins detected in both experiments are shown. Predominantly covalently bound proteins are located in the left segments of the plot. On the y-axis protein abundances in on-bead digested samples with immobilized bioorthogonal moieties relative to unreactive control beads are plotted. Proteins preferentially binding to the reactive groups are located in the upper segments of the plot. c) **Summary of results.** In both experiments a similar number of proteins were detected. These include proteins binding to the matrix as well as those binding to the immobilized compounds. Compound **17** is the only compound for which multiple proteins were found to bind specifically and covalently.

## Figure S2

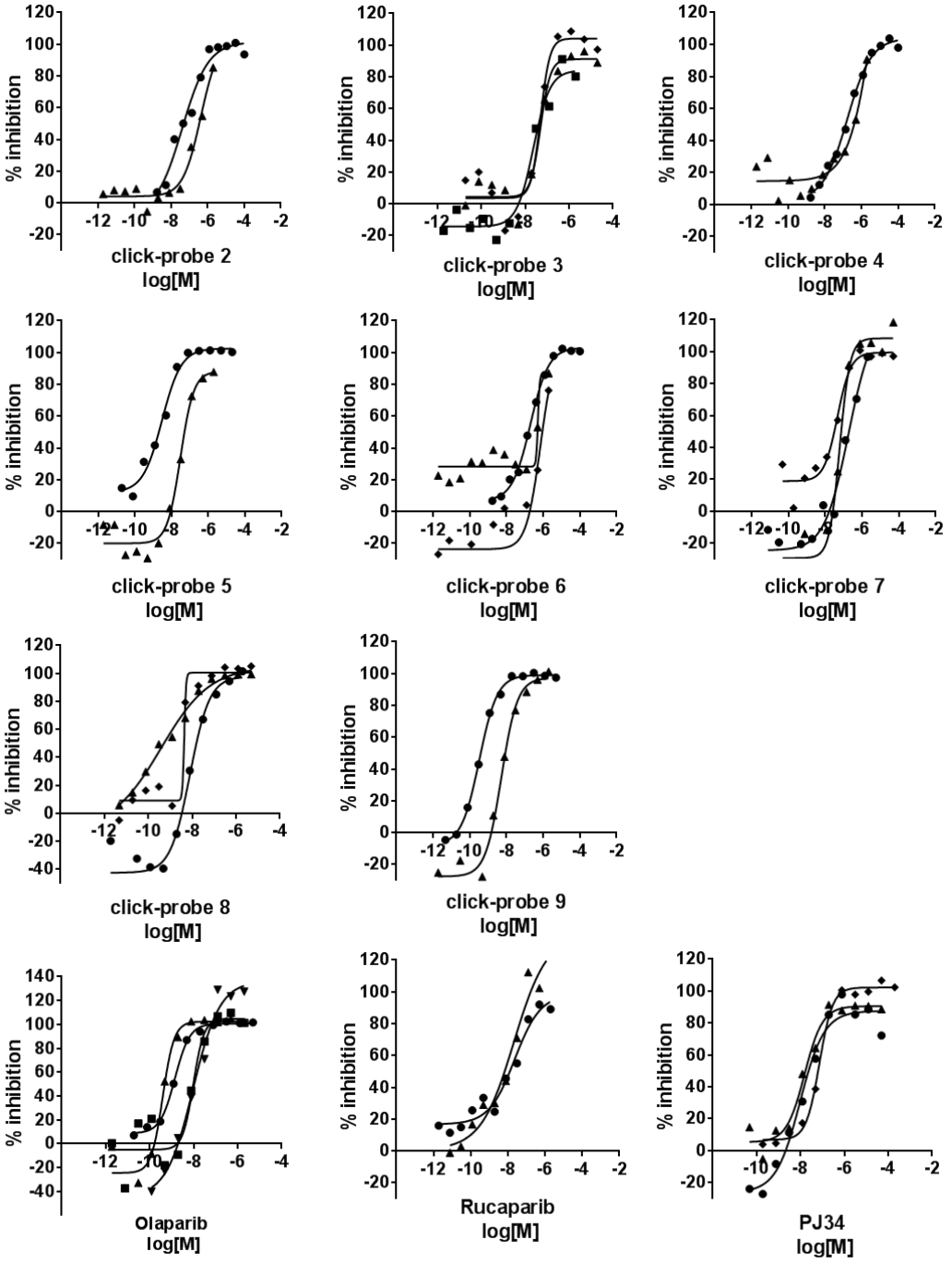


**Figure S2. Affinities of click-probes and inhibitors for endogenous PARP1 evaluated in a lysate-based competition binding assay using sepharose-linked PARP inhibitor.** Competition binding curves for data summarized in Table 1. Chemoproteomics affinity-enrichment assay was performed using an antibody based read-out. The capturing matrix was derivatized with Rucaparib ( see Supplementary Materials for more details).

## Figure S3 – part 1

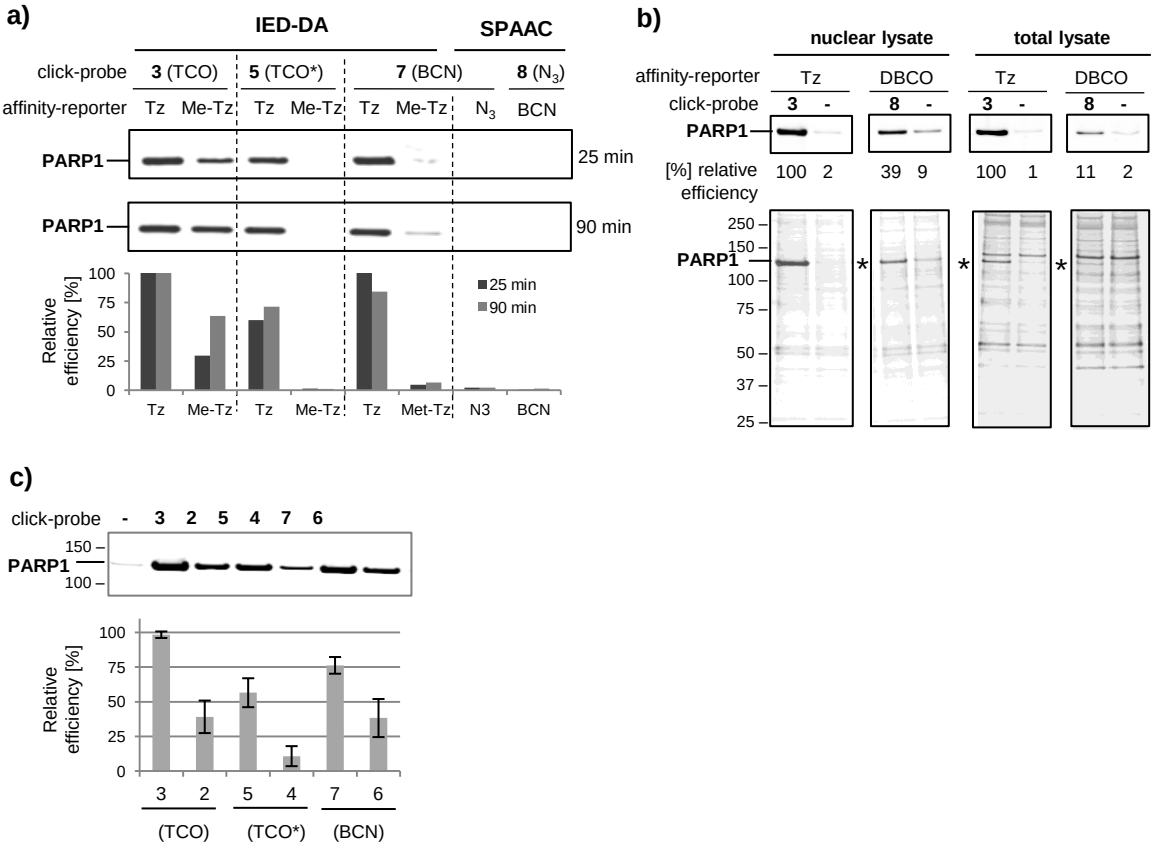


**Figure S3. a) Comparison of the efficiency of IED-DA and SPAAC reactions.** Hela lysates were incubated with different click-probes (1μM) and subsequently neutravidin beads were added, on which the respective bioorthogonal partner group was immoblized. The click reaction was performed for 25 or 90 min at 4°C. Enrichment of PARP1 protein was detected in the eluted fractions via immunostaining. Reported is the relative efficiency of target enrichment as compared to probe 3. **b) Comparison of the two most efficient reactions: IED-DA and SPAAC, in two cellular lystes: nulcear (HuT78) and total (Hela).** Lysates were incubated as described in (a) and click reaction was performed for 45 min at room temperature. Enrichment of PARP1 protein was detected in the elution fractions via immunostaining (upper panel) or silver stain (lower panel, star). Reported is the relative efficiency of target enrichment (based on the western-blot data) as compared to probe 3. **c) Influence of the linker length on the enrichment efficiency (IED-DA probes).** HuT78 or HeLa lysates were incubated as described in (a) and click reaction was performed for 30 min at 4°C. Enrichment of PARP1 protein was detected in the elution fractions via immunostaining. Results for one representative experiment in HuT78 are shown as western blot. Quantification of the data from 4 independent replicates is presented as a graph. Reported is the relative efficiency of target enrichment as compared to probe 3.

## Figure S3 - part 2

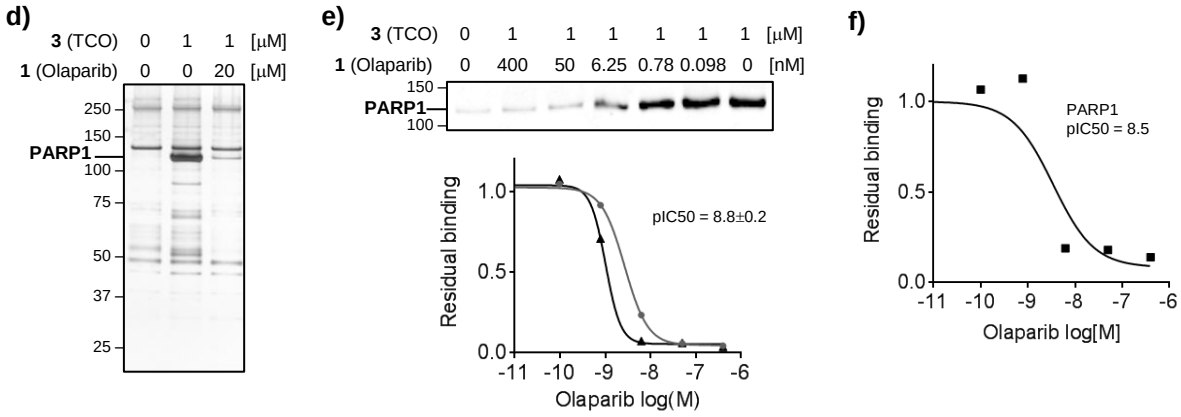


**Figure S3. d)Selectivity profile for Olaparib.** Hela lysate was incubated with click-probe **3** (1 μM) in the presence or absence of Olaparib (20 μM). Specific enrichment of Olaparib targets was performed using the IED-DA reaction between click-probe **3** and biotin-Tz as described before. Elution fractions were analyzed using silver staining. **e) Cellular potency of Olaparib.** Cells were treated with 1μM click-probe **3** in the presence of different concentrations of Olaparib (0-400 nM). After lysis and enrichment using the IED-DA reaction with biotin-Tz coupled streptavidin matrix, samples were analyzed by immunostaining. A western blot of one replicate and competition binding curves for both replicates are shown. **f)** Samples from (d) were also analyzed using mass spectrometry, here a competition binding curve for the second replicate is shown (n=1 shown in Figure 2d).

## Figure S4

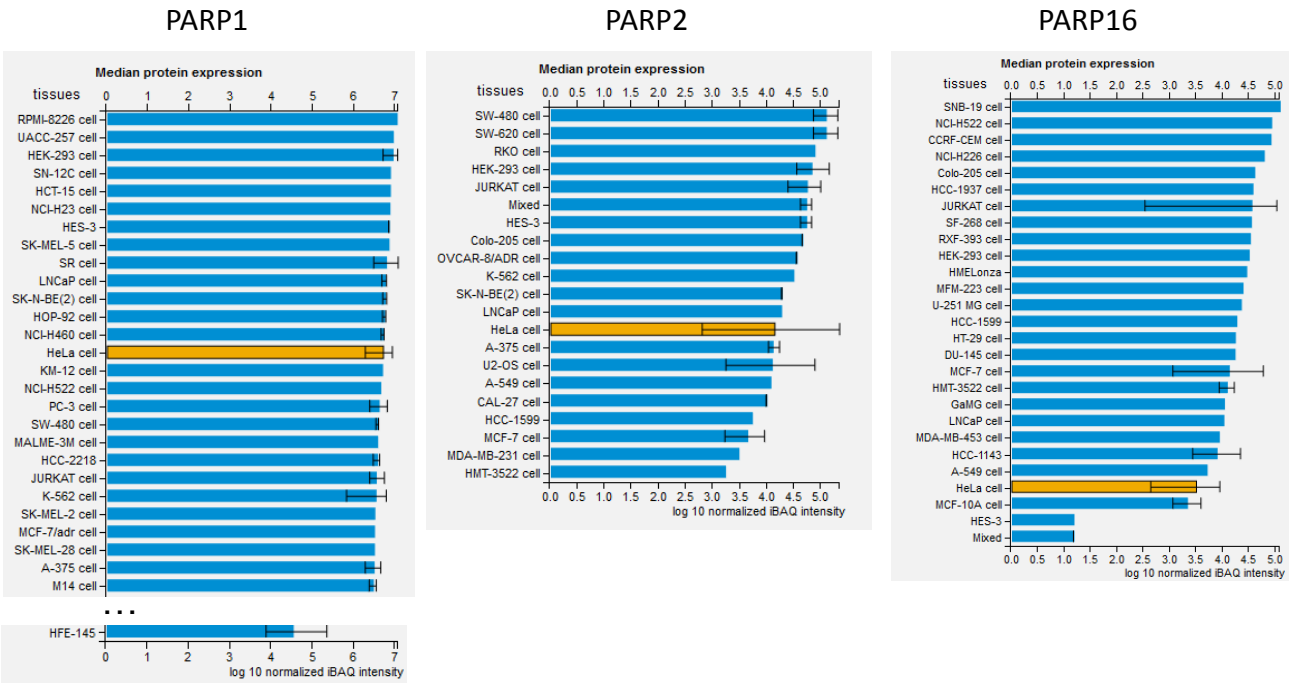


**Figure S4. Expression levels of PARP1, PARP2 and PARP16.** Graphic representation of protein expression levels derived from the data base ProteomicsDB ( https://www.proteomicsdb.org). For PARP1 only the cell lines with highest expression are depicted due to space reasons. The data for HeLa cells (highlighted in yellow) indicates over 100 fold higher expression levels of PARP1 as compared to PARP2 and PARP16.

## Figure S5

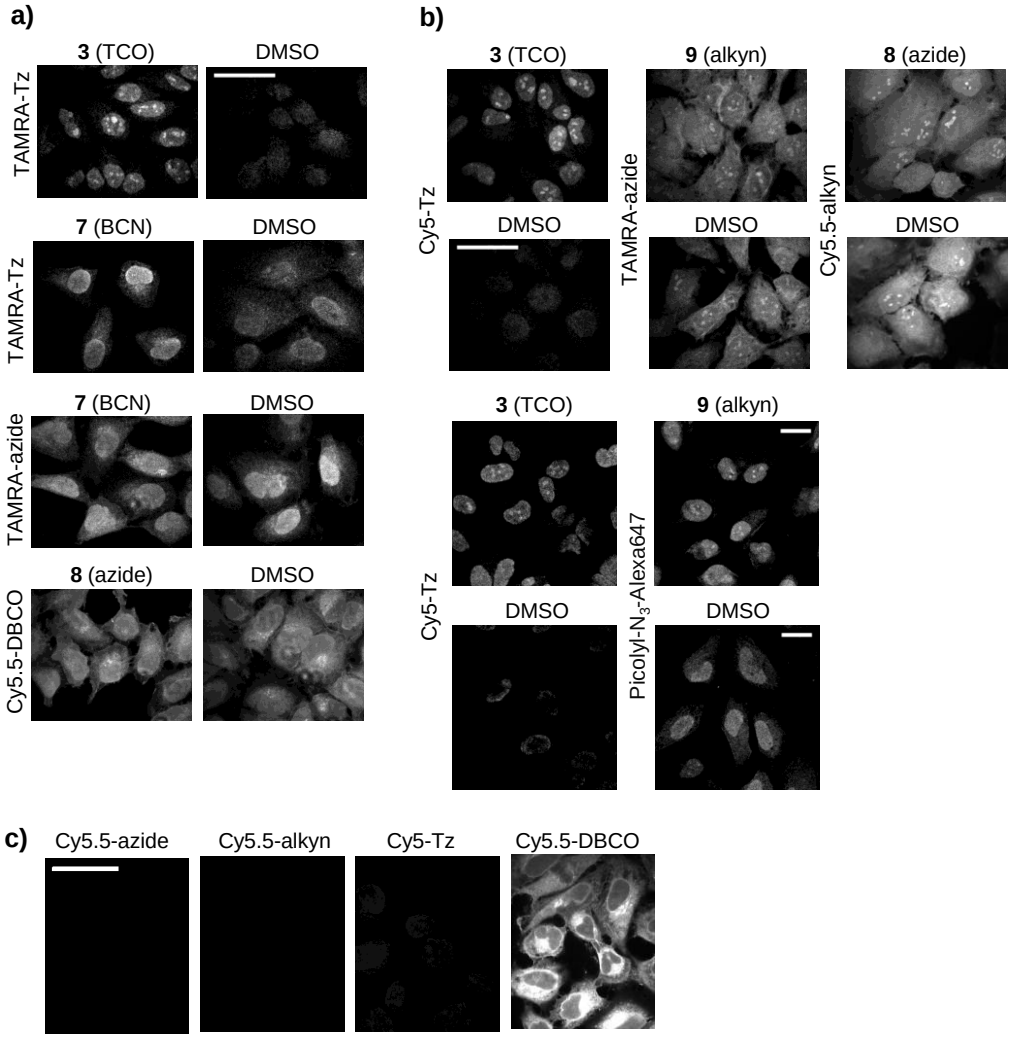


**Figure S5. a) Comparison of IED-DA and SPAAC in the imaging assay**. Fluorescent images of HeLa cells treated with DMSO (right panel) or 2 μM click-probes **3**, **7** or **8** (left panel) for 60 min followed by fixation, permeabilization and click reaction with 100 nM TAMRA-Tz for 5 min or 10 μM TAMRA-azide/Cy5.5-DBCO for 60min. Scale bar = 25 μm. **b) Comparison of IED-DA and CuAAC**. Fluorescent images of HeLa cells treated with DMSO or 2 μM click-probes **3**, **8** or **9** for 60 min followed by fixation, permeabilization and click reaction with 100 nM Cy5-Tz for 5 min or 10 μM TAMRA-azide/Cy5.5-alkyn for 60min. The reaction with Alexa647-Picolyl-azide (Invitrogen) was performed according to supplier manual. Scale bar = 25 μm. **c) Comparison of unspecific reactivity of dye-reporters used for imaging**. Fluorescent images of Hela cells which after fixation and permeabilization were incubated with 1 μM solution of respective dye-reporter for 30min. All images were recorded using the same settings. Scale bar = 25 μm.

## Figure S6

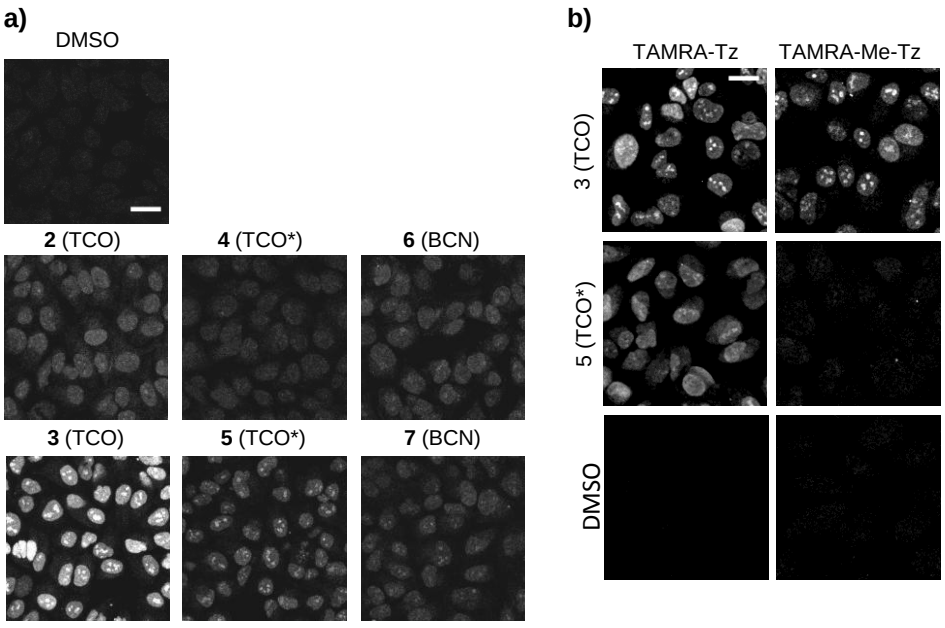


**Figure S6. Compound localization using IED-DA**. a) Fluorescent images (Cy5-channel) of HeLa cells treated with DMSO or 2 µM click-probes **2**-**7** (respectively) for 60 min followed by fixation and click reaction with 100 nM Cy5-Tz for 5min. Scale bar =25 µm. b) Comparison of Tz and Me-Tz in imaging assay. Fluorescent images of HeLa cells treated with 2 µM click-probes **3** or **5** for 60 min followed by fixation and click reaction with 100 nM TAMRA-Tz or 1 µM TAMRA-Me-Tz for 5min. Scale bar = 25 µm.

## Figure S7

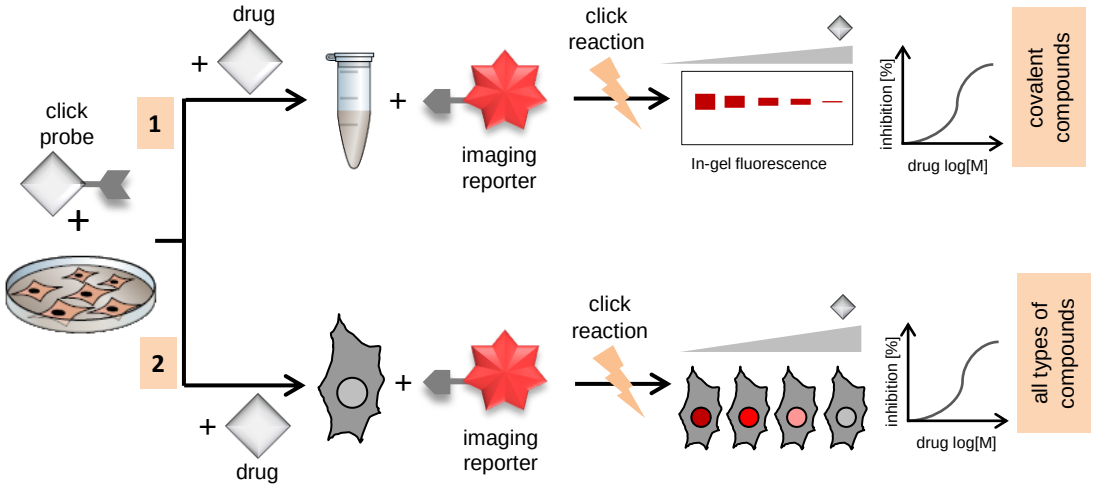


**Figure S7. Two assays for measurement of target occupancy in live cells using dose-depended competition format.** Cells are treated with constant concentration of the click probe as well as dilution array of non-modified drug for which target occupancy will be measured. In case of covalently bound compound (upper panel), cells are then lysed, click reaction with a reporter-dye is performed and samples are analyzed by SDS-PAGE. In-gel fluorescence signal of covalently labeled target is then measured and data are used to calculate $pIC_{50}$ values. Such data represent average over the whole population. In the more general approach (lower panel), applicable to all type of compounds, click reaction with reporter-dye is performed on live or fixed/permeabilized cells enabling visualization and quantification of fluorescently labeled target-probe complexes with single cell resolution.

## Figure S8

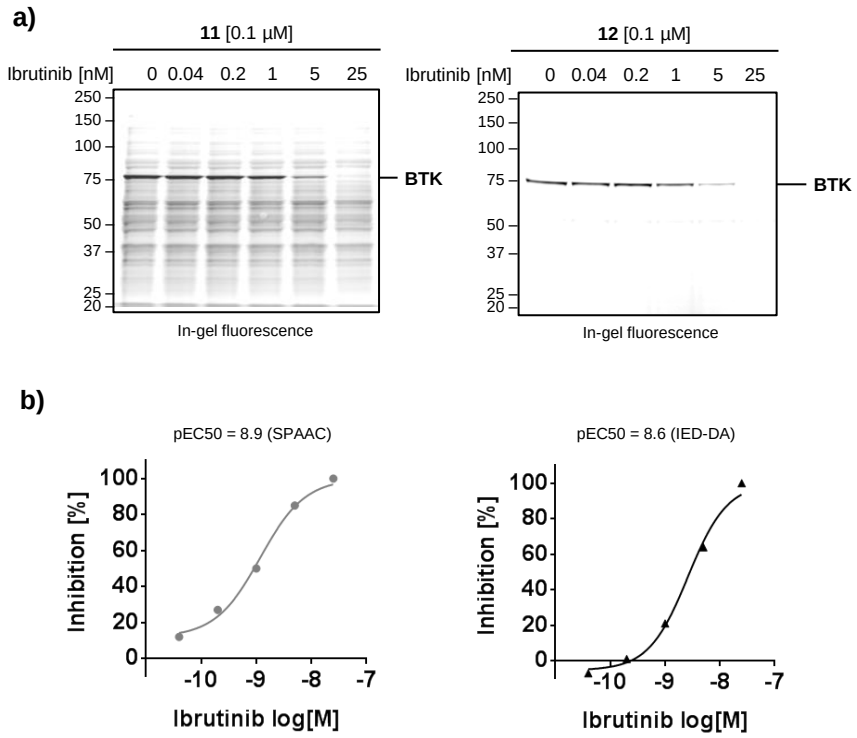


**Figure S8: Target occupancy measurement**. a) In-gel fluorescent scans used for obtaining data shown in Figure 4c. BV173 cells were treated for 60 min with DMSO or 0.1 μM click-probe **11** (left) or click-probe **12** (right) in the presence of different concentrations of Ibrutinib (0 – 25 nM) followed by washing, lysis and in vitro click reaction with either 20 μM Cy5.5-DBCO for 60 min at RT or with 10 μM Cy5-Tz for 30 min at 4°C. Fluorescently labeled proteins were resolved by SDS-PAGE. b) Competition binding curves derived for replicate experiments to the ones described in (a); 0.01 μM of click-probe **11** or 0.1 μM of click-probe **12**.

## Figure S9

a)

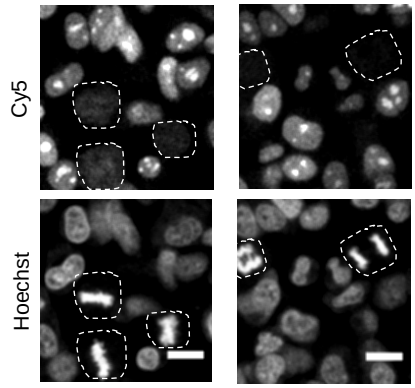


b)

| | Affinity enrichment $pIC_{50}$ in lysate | Microscopy $pEC_{50}$ in cells | FACS $pEC_{50}$ in cells |
|---|---|---|---|
| Olaparib | 8.8± 0.7 | 9.2 ± 0.1 | 8.7 ± 0.1 |
| Rucaparib | 7.7± 0.1 | 8.6 ± 0.2 | 8.0± 0.0 |
| PJ34 | 7.5± 0.5 | 7.3 ± 0.5 | 7.1± 0.1 |

c)

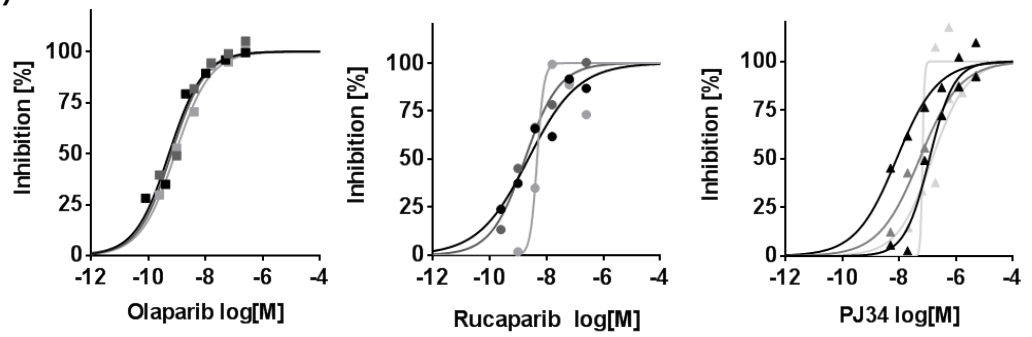


**Figure S9. Cellular target occupancy assays for non-covalent PARP inhibitors.**
a) Fluorescent images of HeLa cells treated with 1 µM click-probe **3** for 60 min followed by fixation, permeabilization and click reaction with 100 nM Cy5-Tz for 5min and Hoechst staining for 10min. Upper panel: excitation at 633 nm (Cy5), lower panel: corresponding image recorded with excitation at 405 nm (Hoechst). Plasma membrane of mitotic cells is marked with dashed line. Scale bar = 15 µm. b) Summary table of $pIC_{50}$ and $pEC_{50}$ values measured in experiments reported in Figure 5. c) Competition binding curves from 3-5 independent experiments described in Figure 5a-c; Olaparib (squares), Rucaparib (circles) and PJ34 (triangles).

## Figure S10

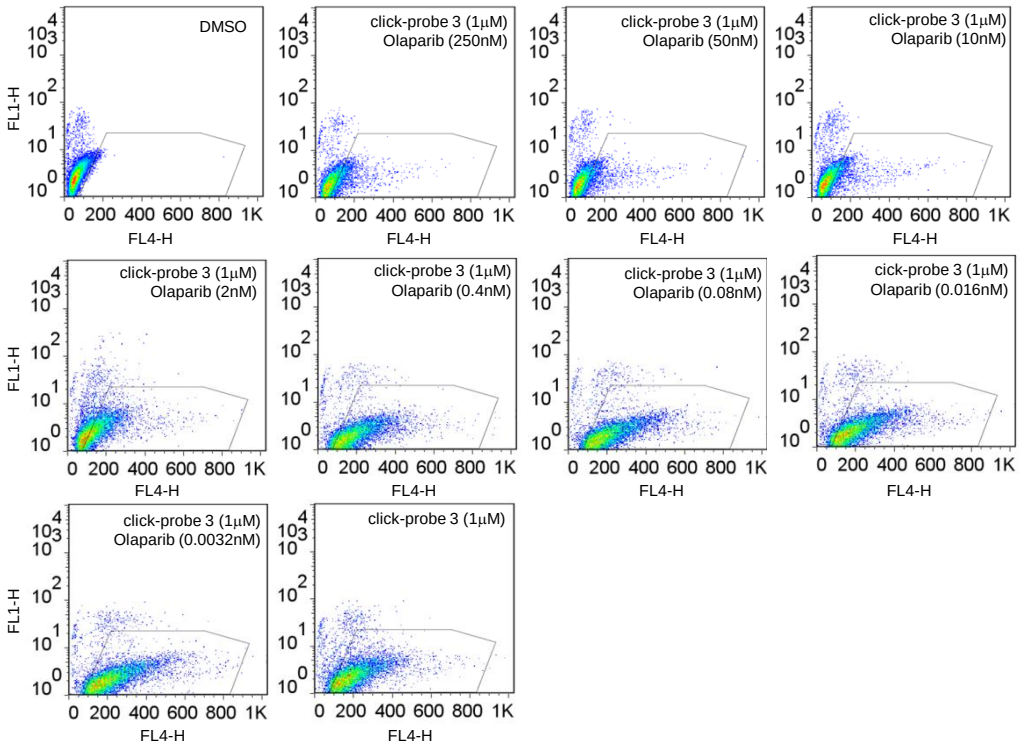


**Figure S10. Cellular target occupancy assays with FACS read-out for PARP inhibitors.**
Scatter plots for one representative competition binding curve for Olaparib from the experiment described in Figure 5d.

## Figure S11

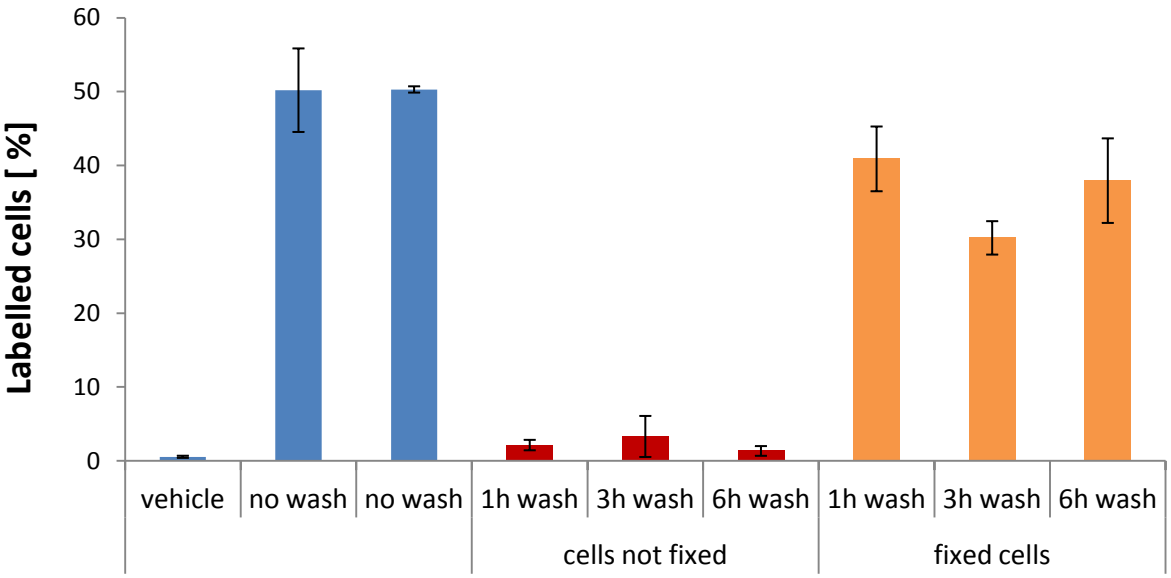


**Figure S11. Cell fixation slows down Olaparib-TCO wash-out.**
Flow cytometric analysis of Jurkat cells treated for 60 min with vehicle or 1 µM click-probe 3. After treatment, cells were shortly washed to remove unbound probe and either directly fixed or incubated with new medium for indicated time (1, 3 and 6 h) prior to fixation. The fixed cells were subjected to wash with PBS after fixation for the same time period (1, 3 and 6 h). Following permeablization, cells were incubated with 100 nM Cy5-Tz for 5 min and click reaction was performed. The bar chart reports one experiment representative of n=2.

## Figure S12

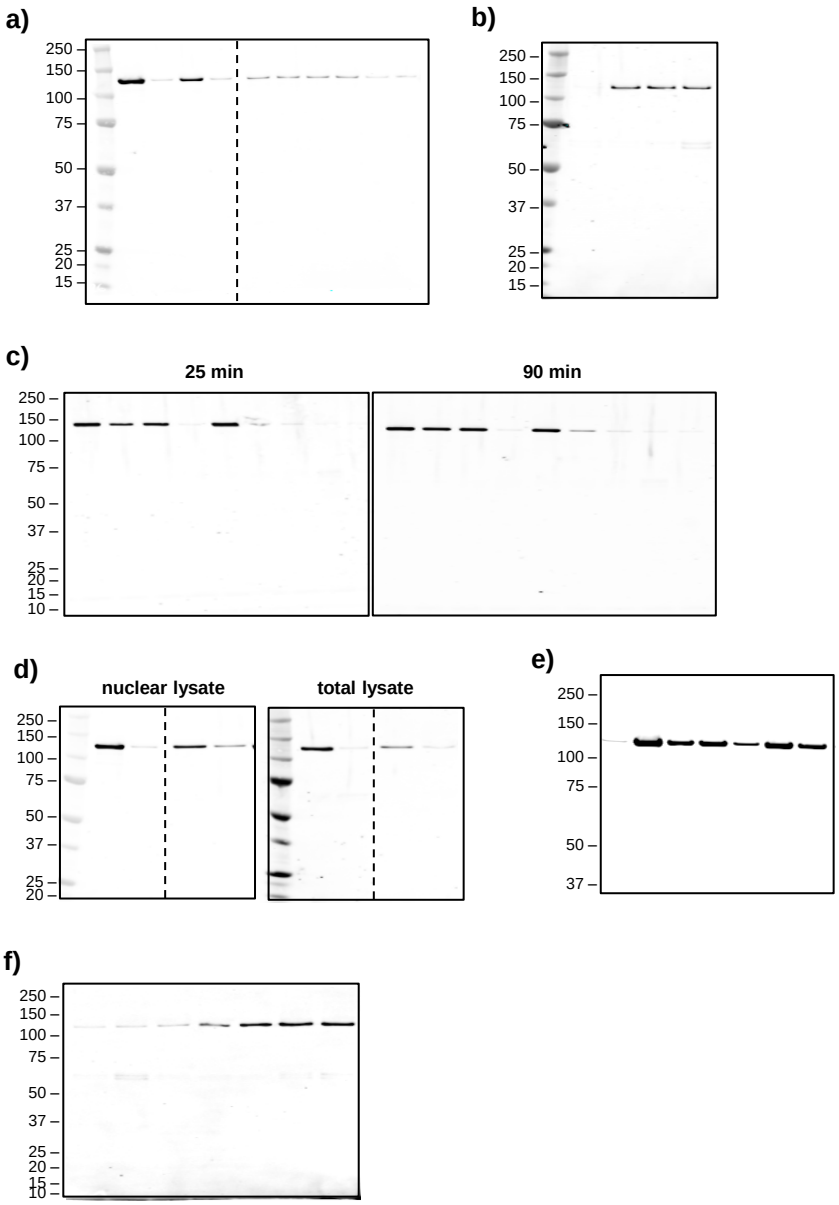


**Figure S12. Full gels for experiments shown in the manuscript.** a) Figure 2a; b) Figure 2c; c) Figure S3a; d) Figure S3b; e) Figure S3c; f) Figure S3e .

## Methods

### Biology

**PARP1 assays.** Chemoproteomics affinity-enrichment assay was performed in a 384-well format using an antibody based read-out. The capturing matrix derivatized with the ligand Rucaparib (AG-014699) was prepared as previously described.[1] Briefly, Rucaparib (Selleckchem) was immobilized on N-hydroxysuccinimide (NHS) activated Sepharose-4 fast flow beads (GE Healthcare) at a final concentration of 0.5 mM. Remaining NHS groups were blocked with ethanolamine. For the assays, 375 µg HeLa lysate and 0.75 µl capturing matrix per well (final volume 75 µl) were incubated in the absence or presence of test compound at 4°C. Each plate contained 16 positive (200 µM PJ34) and 16 negative (2% v/v DMSO) controls. The compounds were tested in a concentration-response format with a starting concentration of 100, 20 or 5 µM applying 1:4 dilution steps for a total of 11 data points. DMSO concentration was 2% (v/v). After 2 h incubation the non-bound fraction was removed by washing the beads with Drug Pulldown (DP) buffer (50 mM Tris-HCl (pH 7.5), 5% (v/v) glycerol, 150 mM NaCl, 1.5 mM MgCl2, 25 mM NaF, 1 mM $Na_3VO_4$, 1 mM dithiothreitol) containing 0.4% (v/v) Igepal-CA630. Proteins retained on the beads were eluted in 2 x SDS sample buffer (100 mM Tris (pH 7.4), 4% (w/v) SDS, 20% (v/v) glycerol, 0.01% (w/v) bromophenol blue, 50 mM dithiothreitol) and loaded on NuPAGE 4-12% Bis-Tris gels (Invitrogen). Electrophoresis was run in MOPS buffer (Invitrogen) for 60 min at 160 V and the proteins were then transferred from the gel to a PVDF membrane. The membranes were incubated with a specific anti-PARP1 antibody (Santa Cruz, sc-25780; 1:200 in PBST, 0.1% Tween) for 18 h at 4°C. After washing steps with PBST at room temperature, membranes were incubated with an IRDye 680–labeled secondary antibody (goat anti-rabbit LiCOR, PIN 925-68071, 1:5000 in PBST) for 1 h at room temperature. Read-out was done using Odyssey Scanner (LI-COR). The data was analyzed using the Graph Pad Prism software (version 6.07). Percentage inhibition was calculated using positive and negative controls as 100% and 0% inhibition, respectively. Concentration-response curves were fitted using a four-parameter non-linear regression fitting module.

**Precoupling of Streptavidin beads with biotinylated bioorthogonal compound** (**13**-**15**, **17**-**18**). High-capacity streptavidin agarose beads (Thermo Scientific) were pre-coupled with biotinylated bioorthogonal compounds. 200 µl of beads (400 µl of 50% slurry) were washed 2 times with DP buffer containing 0.4% (v/v) Igepal-CA630 and cOmplete EDTA-free protease inhibitor cocktail (Roche). Then, 1.33 µL or 3.33 µl of respective biotin-compound (**13**-**15**, **17**-**18**, 30mM stock in DMSO) were added to the beads (for a coupling density of 0.2mM or 0.5mM) and incubated for 30 min at 4°C under overhead rotation. The beads were then washed twice with DP buffer and resuspended in 5 X beads volume of DP buffer to make a 20% slurry. For mass spectrometry read-out, an additional blocking step with free Biotin was performed to decrease the unspecific binding to the bead surface. After incubation with Biotin-Tetrazine, 2 µl free Biotin (1mM final concentration) were added to the beads for 30 min at 4°C under overhead rotation, then the beads were washed as described above.

**In-lysate PARP1 pull-down with IED-DA.** HeLa total lysate was diluted to 1.5 mg/ml in DP buffer and the concentration of Igepal-CA630 was adjusted to 0.4%. The lysate was then ultracentrifuged at 33500 rpm for 20 min at 4°C. 1 µl of respective compound (**2**-**7**, 1 µM final concentration) and 1 µl Olaparib for competition (10-20 µM final concentration) were added to 200 µl of lysates, and the samples were incubated for 1 h at 4°C under overhead rotation. A 96-well filter plate (Millipore) was washed with 200 µl DP buffer and in each well 15 µl of pre-coupled tetrazine beads (75 µl beads

slurry, Biotin-Tetrazine, compound **13**, 0.2 mM coupling density) were loaded onto the plate. The plate was centrifuged at 500 rpm for 15 sec to remove the buffer and 120 µl of treated lysate was added to the beads. The plate was then incubated for 30 min at 4°C with shaking (650 rpm) and afterwards centrifuged at 1200 rpm for 1 min. The non-bound fractions were discarded and the plate was washed three times with DP buffer. Then 75µL of elution buffer (2X-LDS sample buffer (Invitrogen) supplemented with 50mM DTT) was added to the beads and plates were incubated for 30min at room temperature with shaking (650 rpm). The plate was then centrifuged for 2 min at 1200 rpm and the elution fractions were collected into a 96-well plate. The samples were separated on NuPAGE 4-12% Bis-Tris gels (Invitrogen) and the proteins were then transferred to a PVDF membrane and PARP1 was detected as described above using anti-PARP1 antibody (Santa Cruz, sc-25780). For silver staining, the Pierce Silver Stain kit (Thermo Scientific) was used following the manufacturer's instruction. For LC-MS/MS analysis the protocol was scaled-up to 120 µl of 5mg/ml Hela lysate and 35 µl of beads per condition. The eluates were reduced, alkylated and separated on SDS-PAGE as described below.

**In-lysate PARP1 pull-down with SPAAC.** The protocol was similar to the in-lysate pull-down with IED-DA with a few exceptions: HeLa total or HuT78 nuclear lysates were incubated first with compound **8**, and later with pre-coupled DBCO or BCN beads (DBCO-Biotin (760749 Sigma Aldrich), BCN-Biotin compound **17**, 0.5mM coupling density) for 45 min at room temperature.

**In-lysate PARP1 pull-down with CuAAC ($CuSO_4$/THPTA/Sodium ascorbate).** HuT78 nuclear lysate was diluted to 3 mg/ml as described above. 1 µl of compound **8** or **9** at 1 µM final concentration was added to 250 µl lysate and the samples were incubated for 1 h at 4°C under overhead rotation. A 96-well filter plate (Millipore) was washed with 200 µl DP buffer and in each well 15 µl of beads precoupled to either compound **18** or **15** (75 µL beads slurry, 0.5 mM coupling density) were added. The plate was centrifuged at 500 rpm for 15 sec to remove the buffer and 120 µl of treated lysate was added to the beads. Then a mixture (prepared freshly shortly before use) of $CuSO_4$ (0.2 mM), THPTA (1 mM), sodium ascorbate (2 mM) in water were added to the samples. The plate was incubated for 90 min at RT with shaking (650 rpm) and then centrifuged at 1200 rpm for 1 min in order to discard the non-bound fractions. The washing, elution from the beads, gel electrophoresis and western blot were performed as described above.

**In-lysate PARP1 pull-down with CuAAC ($CuSO_4$/TBTA/TCEP).** Protocol was based on that previously described.[2] The same experiment as described above was repeated with different reagents: $CuSO_4$ (1mM), TBTA (0.1 mM, stock solution of 1.7 mM in DMSO/$^t$BuOH, 1:4 v/v ) and TCEP (1 mM). The Solution of the three reagents in water was prepared shortly before use in following order: $CuSO_4$ and TBTA were mixed together and then TCEP added. However, upon addition of this solution to lysates a formation of a white precipitate was observed, which was aggregating on the filter plate and made the next steps not possible.

**Cellular treatment followed by PARP1 pull-down with IED-DA.** HeLa cells were grown to 80-90% confluency on a 10-cm plate in RPMI medium supplemented with 10% fetal bovine serum (FBS), 1 mM sodium pyruvate and non-essential amino-acids. The media was then removed and replaced with 7.5 ml media containing 1 µM compound **3** and different concentrations of Olaparib (compound **1**) (1 vehicle control / DMSO + 5 concentrations; 400nM – 0.098nM; dilution: 1/8). After incubation in a humidified 37°C, 5% $CO_2$ incubator for 1 h, the cells were washed twice with 10 ml of media with 5 min incubation between each step. The media was then aspirated, cells collected in 4 ml PBS

(scraping) and peletted by centrifugation at 1000 rpm for 3 min at room temperature. Cells were resuspended in 1 ml DPBS, transferred to a 1.5 mL eppendorf tube and pelleted again at 1000 rpm for 3 min. Cell pellets were then resuspended in DP buffer supplemented with protease inhibitor cocktail and 0.8% (v/v) Igepal-CA630 and shaken at 900 rpm for 30 min at 4°C. Lysates were then ultracentrifuged at 100,000 g for 1 h at 4°C. The supernatant was collected and the protein concentration was determined using the Bradford assay (Bio-Rad). All lysates were diluted individually with DP buffer to achieve a protein concentration of 1.5 mg/ml. The concentration of Igepal-CA630 was adjusted to 0.4%. The pull-down procedure was performed as described above for in-lysate pull-down, including the following modifications: 350 µL lysate, 3.7 µl beads, 50 µl elution buffer and elution at 50°C. Eluates were separated on SDS-PAGE and analyzed as described above for immunostaining. For LC-MS/MS analysis eluates were alkylated, separated on SDS-PAGE and proceeded as described below.

**Visualization of PARP1 inhibitors in cells (imaging).** HeLa cells were allowed to grow to 80–90% confluency on a 8-well Labtek tissue culture dish in MEM medium supplemented with 1% puryvat, 1 % NAA and 10% FBS. The medium was then removed and cells were treated with media containing compound **2**-**9** at indicated concentrations (usually 1-2µM). The cells were incubated in a humidified 37 °C, 5% $CO_2$ incubator for 60 min. The medium was then removed and the cells were washed 3 times with fresh medium and once with PBS to remove unbound compound. The cells were then fixed in 4% paraformaldehyde in PBS for 10min, washed 3 times with PBS and finally permeabilized with 0.5% Triton in PBS. After 3 washes with PBST (0.1% Tween in PBS), respective bioorthogonal reaction with reporter-dye was performed at RT. (a) IED-DA reaction: cells were incubated with 100 nM Tetrazine-Cy5, 100 nM Tetrazine-TAMRA or 1µM 6-methyl-Tetrazine-TAMRA (all Jena Bioscience) for 5 min at RT. (b) SPAAC reaction: cells treated with compound **7** were incubated with Azide-5-TAMRA (Jena Bioscience) for 1-60 min at RT, concentration tested 0.1-50 µM; cells treated with compound **8** were incubated with 10 µM DBCO-Cy5.5 (Jena Bioscience) for 5-60 min. (c) CuAAC reaction: to dishes treated with compound **9**, a mixture containing Azide-5-TAMRA (Jena Bioscience) at 5-50 µM and $CuSO_4$/THPTA/sodium ascorbate (5 mM/1 mM/10 mM or 0.5 mM/0.1 mM/1 mM, respectively) in PBS was added to the samples for 60 min. Alternatively, bioorthogonal reaction was performed using Click-iT Plus Alexa 647 Picolyl Azide Kit (Life Technologies) following the manufacturer's protocol. Cells treated with compound **8** were processed as described above but Alkyne-Cy5.5 (Jena Bioscience) was used instead of Azide-5-TAMRA. For both CuAAC and SPAAC reactions blocking with 3% BSA (in PBS with 0.3% saponin) prior to bioorthogonal reaction was also tested to decrease unspecific background. After bioorthogonal reaction, the cells were washed 5 times with PBST and Hoechst staining was performed for 10min at RT. Finally, dishes were washed 2 times with PBST and once with PBS and imaged directly. The image acquisitions were carried out using a Zeiss LSM 780, Zeiss LSM 780 NLO or PE Ultraview ERS microscopes using 40x or 63x oil objectives. The data was analyzed using ImageJ.

When indicated, an immunostaining was performed directly after the bioorthogonal reaction. The cells were blocked with 3% BSA in PBST for 1 h, then anti-PARP1 antibody (Abcam, ab6079) in 1% BSA in PBST was added and dishes were incubated at 4°C overnight. After 3 washes with PBST (0.1% Tween in PBS), secondary antibody solution (Alexa 488, anti-rabbit) containing Hoechst in 1% BSA in PBST was added and dishes were incubated at RT for 1 h. Finally, cells were washed 3 times with PBST, once with PBS and directly imaged.

**Cellular target occupancy measurement for PARP1 inhibitors using microscopy read-out.** Experiments were performed accordingly to protocol described above but cells were treated with media containing compound **3** (1 µM final concentration) and either the respective inhibitor or 0.1% DMSO. The inhibitors were tested in a concentration-response format with a starting concentration of 0.25 µM (Rucaparib and Olaparib) or 5 µM (PJ34) applying 1:4 dilution steps for in total 6 data points. In general, 6 to 8 images were recorded per well/condition and the data was analyzed using the ImageJ and the CellProfiler software. In short, Hoechst staining was used to define the area of each nucleus and this mask was then overlaid on the Cy5 channel to quantified mean fluorescent intensity of labeled compound per nucleus. $pIC_{50}$ values were calculated using the Graph Pad Prism software version 6.07 as described above for the Parpobeads. For each inhibitor at least 3 independent experiments were performed.

**Cellular target occupancy measurement for PARP1 inhibitors using Fluorescence Activated Cell Sorting.** $1x10^6$ cells per sample were collected by centrifugation at 1500 rpm for 3 min at room temperature. Pellets were then resuspended in 0.2 ml of media containing compound **3** (1 µM final concentration) and either the respective inhibitor or 0.1% DMSO. The inhibitors were tested in a concentration-response format with a starting concentration of 0.25 µM (Olaparib), 1.25 µM (Rucaparib) and 10 µM (PJ34) applying 1:5 dilution steps for a total of 8 data points. After incubation at 37 °C for 60 min, the cells were washed three times with fresh media before a final wash in PBS. The cells were then fixed for 10 min at RT with 4% PFA followed by permeabilisation with 0.5% Triton X-100 in PBS for 5 min with 2-3 vortexing steps in-between. Cells were subsequently incubated with 100 nM Cy5-Tz dye (Jena-Bioscience) for 5 min at RT with 2-3 vortexing steps in between followed by 5 washing steps with PBST (PBS with 0.1% Tween20). The cells were then subjected to flow cytometric analysis using a FACSCalibur instrument (BD Biosciences, San Jose, CA). A total of 20,000 events was collected for each sample, and the forward- and side-scatter properties were used to exclude doublets, dead cells, and debris. Cells were excited with a red laser (635 nm) and Cy5 fluorescence was detected using a 660/20 band pass filter (FL4-H channel). A gate for Cy5-positive cells was defined in a FL1-H/FL4-H scatter plot (FL1-H detecting cell autofluorescence), and the percentage of Cy5-positive cells among all cells was calculated based on the number of events recorded within that gate. The data were analyzed using GraphPad Prism as described above for the Parpobeads. The error bars represent standard deviations from two independent replicates.

**In-lysate fluorescent labeling of BTK with IED-DA.** BV-173 total lysate was diluted to 2 mg/mL in DP buffer supplemented with cOmplete EDTA-free protease inhibitor cocktail (Roche) and the concentration of Igepal-CA630 was adjusted to 0.4%. The lysate was then ultracentrifuged at 33,500 rpm for 20 min at 4°C. 1 µL compound **12** (0.1 µM final concentration) and 1 µl Ibrutinib (compound **10**) (5 µM final concentration) were added to 400 µL lysate, and the samples were incubated for 1 h at 37°C under overhead rotation. 1 µl of Tetrazine-Cy5 (Jena Bioscience, 10 µM final concentration) was then added to 49 µL of treated lysate and samples were incubated for 30 min at 4°C in the dark. 50 µl of 2X-LDS sample buffer supplemented with 50 mM DTT was then added to the samples and they were heated at 95°C for 5 min. The samples were separated on NuPAGE 4-12% Bis-Tris gel (Invitrogen). The gel was imaged with using a LiCOR Odyssey scanner for in-gel fluorescence read-out and subsequently stained with Coomassie Blue.

**In-lysate fluorescent labeling of BTK with SPAAC.** The BV-173 lysate was diluted and treated with compound **11** and Ibrutinib (**10**) as described in previous experiment. After compound treatment, the lysate was incubated with iodoacetamide (Sigma, 15mM final concentration) for 30 min at room

temperature in the dark. 1 µL of DBCO-Cy5.5 (Jena Bioscience, 10 µM final concentration) was then added to 49 µl of treated lysate and samples were incubated for 45 min at room temperature in the dark. The samples were diluted in 2X-LDS sample buffer, analyzed by SDS-PAGE and gels were imaged as described above.

**Cellular target occupancy measurement for Ibrutinib**. BV-173 cells were grown in RPMI-1640 medium supplemented with 10% FBS. $2.8x10^8$ cells were centrifuged for 5 min at 1500 rpm, at RT and the cell pellet was resuspended in 50.4 ml RPMI-1640 medium supplemented with 0.1% FBS. 3.6 ml of cell suspension ($2x10^7$ cells) was transferred to each well of two 6-well cell culture plates. Ibrutinib (**10**, final concentration: 0.04 – 25 nM, 1/5 dilutions) or DMSO prepared in RPMI-1640 medium with 0.1% FBS (0.25% DMSO final concentration) was added to each well (in duplicate) and cells were incubated for 1 h at 37 °C, 5% $CO_2$ with horizontal shaking (100 rpm). Subsequently, compound **11** (at 0.1 µM or 0.01 µM final concentration) or compound **12** (at 0.1 µM final concentration) was added. The cells were incubated for additional hour at 37 °C, 5% $CO_2$, with shaking (100 rpm). After incubation, cells were transferred to 15 ml tubes containing 10 ml ice cold PBS and cells were collected by centrifugation for 4 min, 1500 rpm, 4 °C. The cell pellets were then washed two more times with 10 ml ice cold PBS. Finally, cells were lyzed by adding 2 pellet volumes of lysis buffer (HEPES buffer / 0.8% Igepal-CA630 / Protease inhibitor) and resuspending 20 times using a 200 µl pipette tip. Lysates were then incubated for 30 min at 4 °C with shaking (10 rpm) and subsequently ultracentrifuged at 100,000 x g for 30 min at 4 °C. The supernatant was collected and protein concentration was determined using Bradford assay. All lysates were individually diluted with HEPES buffer to get a protein concentration of 2 mg/ml. For SPAAC reaction (compound 11): to each of these lysates iodoacetamide at a final concentration of 15 mM was added followed by incubation for 30 min, at room temperature, in the dark. Subsequently, Cy5.5-DBCO (Jena Bioscience #CLK-1046-1) was added at a final concentration of 20 µM and smaples were incubated for 1 h (room temperature, in the dark). For IED-DA reaction (compound 12): to each lysate Cy5-Tz (Jena Bioscience) was added at a final concentration of 10 µM and smaples were incubated for 30min at 4°C. Afterwards, 30 µl of 2X-LDS sample buffer supplemented with 50 mM DTT was added to 30 µl sample and the samples were incubated for 5 min at 95 °C. 20 µl of each sample was separated on NuPAGE 4-12% Bis-Tris gel (Invitrogen) and gels were then imaged using a LiCOR Odyssey scanner as described above. Signal intensities of fluorescently labeled BTK were quantified and data were analyzed using the Graph Pad Prism software (V6.07) as described above for the Parpobeads. Subsequently, the proteins in the gel were fixed (2% acetic acid in 40% ethanol) and stained with Coomassie Blue.

**Reactivity of bioorthogonal groups in lysate (MS).** High-capacity streptavidin agarose beads (Thermo Scientific) were pre-coupled with biotinylated compounds **13-17, 19-20** (coupling density of 0.45 mM) as described above. The follow-up procedure was similar to the one for the in-lysate PARP1 pull-down but the beads (35ul per condition) were incubated with K-562 total lysate (5 mg/ml) at 4°C or 25°C for 2 hours. Non-covalently bound proteins were eluted with the 2x SDS elution buffer, reduced, alkylated and separated on SDS-PAGE as described below. To assess the covalently bound proteins, the beads (after elution of the none covalently bound proteins) were washed batch wise with 1 time 5ml 2% SDS, 3 times 10 ml 8 M Urea and 4 ml 2 M Urea in 50 mM TEAD. The beads bound proteins were reduced and alkylated with DDT and IAA followed by a tryptic digestion in TEAB.

**Mass Spectrometry**

**Sample preparation for mass spectrometry.** Eluates from beads were concentrated on NuPAGE 4-12% Bis-Tris Midi gels (Invitrogen) by running samples approximately 2 cm into the gel. After staining with colloidal Coomassie, gel lanes were cut into three slices covering the entire separation range (~2 cm) and subjected to in-gel digestion.[1] The fractions covalently bound to the bead matrix were processed as described above.

Afterwards, peptide samples were labeled with 10-plex TMT (TMT10, Thermo Fisher Scientific) reagents, enabling relative quantification.[3] The labeling reaction was performed in 40 mM triethylammoniumbicarbonate, pH 8.53 at 22°C and quenched with glycine. Labeled peptide extracts were combined to a single sample per experiment.

**LC-MS/MS analysis.** Samples were dried *in vacuo* and resuspended in 0.05% trifluoroacetic acid in water. Samples were injected into an Ultimate3000 nanoRLSC (Dionex, Sunnyvale, CA) coupled to a Q Exactive (Thermo Fisher Scientific). Peptides were separated on custom 50 cm × 100 µM (ID) reversed-phase columns (Reprosil) at 40°C. Gradient elution was performed from 2% acetonitrile to 40% acetonitrile in 0.1% formic acid over 2 h. Samples were online injected into Q-Exactive mass spectrometers operating with a data-dependent top 10 method. MS spectra were acquired by using 70.000 resolution and an ion target of 3E6. Higher energy collisional dissociation (HCD) scans were performed with 35% NCE at 35.000 resolution (at m/z 200) and the ion target settings was set to 2E5 so as to avoid coalescence.[4] The instruments were operated with Tune 2.2 or 2.3 and Xcalibur 2.7 or 3.0.63.

**Peptide and protein identification.** Mascot 2.4 and 2.5 (Matrix Science) was used for protein identification by using a 10 parts per million mass tolerance for peptide precursors and 20 mD (HCD) mass tolerance for fragment ions. Carbamidomethylation of cysteine residues and TMT modification of lysine residues were set as fixed modifications and methionine oxidation, and N-terminal acetylation of proteins and TMT modification of peptide N-termini were set as variable modifications. The search database consisted of a customized version of the International Protein Index protein sequence database combined with a decoy version of this database created by using a script supplied by Matrix Science. Unless stated otherwise, we accepted protein identifications as follows: (i) For single-spectrum to sequence assignments, we required this assignment to be the best match and a minimum Mascot score of 31 and a 10× difference of this assignment over the next best assignment. Based on these criteria, the decoy search results indicated <1% false discovery rate (FDR). (ii) For multiple spectrum to sequence assignments and using the same parameters, the decoy search results indicate <0.1% FDR. All identified proteins were quantified; FDR for quantified proteins was <1%.

**Peptide and protein quantification.** For the analysis a in house version of isobarQuant[5] was used. Reporter ion intensities were read from raw data and multiplied with ion accumulation times (the unit is milliseconds) so as to yield a measure proportional to the number of ions; this measure is referred to as ion area.[6] Spectra matching to peptides were filtered according to the following criteria: mascot ion score >15, signal-to-background of the precursor ion >4, and signal-to-

interference >0.5.[7] Fold-changes were corrected for isotope purity as described and adjusted for interference caused by co-eluting nearly isobaric peaks as estimated by the signal-to-interference measure.[8] Protein quantification was derived from individual spectra matching to distinct peptides by using a sum-based bootstrap algorithm; 95% confidence intervals were calculated for all protein fold-changes that were quantified with more than three spectra.[6] Relative protein abundances were generated on the basis of MS1 abundances.[9,10] Briefly, XIC peaks were matched to identified peptides. The apex of the XIC peak was acquired to be within 30 sec from the time of the MS2 event performed on the peptide precursor. The raw abundances of the XIC peaks of the peptides with identical sequences were summed (i.e. same sequence, but different charge states and/or different modifications), and the resulting single entity was referred to as a sequence. For each protein the 3 sequences with the highest raw XIC intensity from a given sample were selected and log 10 transformed. These values were then summed, and the mean was calculated. In cases where fewer than 3 sequences were associated, the mean was calculated using XIC intensities from either one or two sequences. For the analysis in figure S1 the proteins were filtered for more than one qupm (unique peptide matches used for quantification) and for the MS1 abundances the spread of the top 3 peptides had to be less the 0.6. In order to calculated differences in the MS1 abundance for proteins identified only in one of the two samples the value was set to the lowest obtained in the data set. For the analysis in figure 2B the proteins were filtered for more than two qupm and for the MS1 abundances the spread of the top 3 peptides had to be less the 0.6. For the analysis in figure 2D and S2E the proteins were filtered for more than one qupm.

**pIC50 calculations.** For chemoprotoemic dose response experiments, the vehicle condition was used as the reference for fold-change calculation. Sigmoidal dose-response curves were fitted by using R (www.r-project.org) and the drc package (www.bioassay.dk) as previously described (1).

**Chemistry**

**General.**

All solvents and chemicals were used as purchased without further purification. For separation of DCM and aqueous layers during sample workup Radleys Phase Separation 6ml Columns (RR99821) were used. Preparative high performance liquid chromatography (preparative HPLC) was performed on a waters auto purification system [2767 Sample manager, 2545 Binary Gradient Module, 2420 ELS Detector, 2996 Photodiode Array Detector, 3100 Mass Detector, Waters SFO, Waters 515 HPLC Pump]. The purification was done on a XBridge BEH C18 OBD 5µm Prep Column using a water/acetonitrile mixture (0.2% formic acid as modifier) at a flow rate of 30 mL/min. The purity of all final compounds was 95% or higher unless stated as determined by ultra performance liquid chromatography (UPLC), photodiode array detection. The instrument used for analysis was a waters Acquity system [detectors: Acquity SQD, Acquity ELSD, Acquity PDA] with a waters ACQUITY UPLC BEH C18 1.7 µm Column. The analysis was performed at a flow rate of 1 mL/min with a linear gradient over 2 min (3 to 99% acetonitrile in water, 0.1% formic acid as modifier). Proton ($^1$H) NMR spectra were recorded on a Bruker Avance 400 spectrometer (400 MHz) using DMSO-$d_6$ or $CDCl_3$ as solvents. Chemical shifts are given in parts per million (ppm) (δ relative to residual solvent peak for $^1$H).

***N*-(2-aminoethyl)-5-(4-(2-fluoro-5-((4-oxo-3,4-dihydrophthalazin-1-yl)methyl)benzoyl)piperazin-1-yl)-5-oxopentanamide**

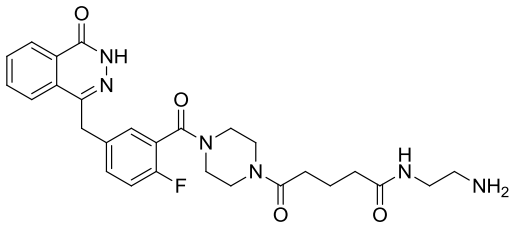

*N*-(2-aminoethyl)-5-(4-(2-fluoro-5-((4-oxo-3,4-dihydrophthalazin-1-yl)methyl)benzoyl)piperazin-1-yl)-5-oxopentanamide was synthesized as described.[11,12]

**5-(4-(2-fluoro-5-((4-oxo-3,4-dihydrophthalazin-1-yl)methyl)benzoyl)piperazin-1-yl)-5-oxopentanoic acid**

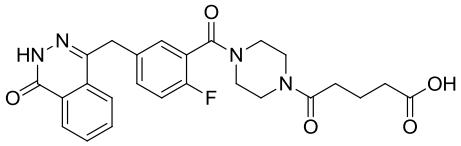

5-(4-(2-fluoro-5-((4-oxo-3,4-dihydrophthalazin-1-yl)methyl)benzoyl)piperazin-1-yl)-5-oxopentanoic acid was synthesized as described.[11,12]

**4-(4-fluoro-3-(piperazine-1-carbonyl)benzyl)phthalazin-1(2*H*)-one**

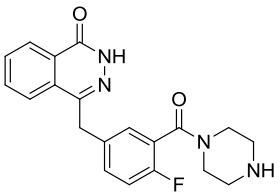

4-(4-fluoro-3-(piperazine-1-carbonyl)benzyl)phthalazin-1(2*H*)-one was synthesized as described.[13]

**4-(3-(4-(cyclopropanecarbonyl)piperazine-1-carbonyl)-4-fluorobenzyl)phthalazin-1(2*H*)-one** (**1**)

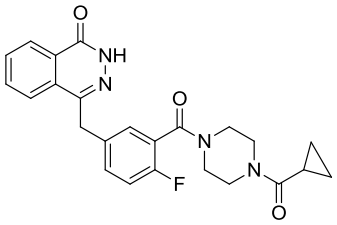

4-(3-(4-(cyclopropanecarbonyl)piperazine-1-carbonyl)-4-fluorobenzyl)phthalazin-1(2*H*)-one was purchased from ChemScence as used as received.

**(*E*)-cyclooct-4-en-1-yl-4-(2-fluoro-5-((4-oxo-3,4-dihydrophthalazin-1-yl)methyl)benzoyl)piperazine-1-carboxylate** (**2**)

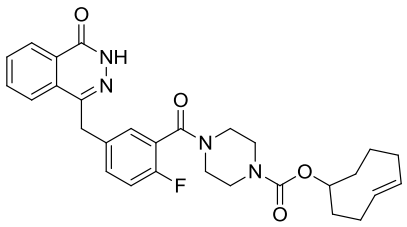

4-(4-fluoro-3-(piperazine-1-carbonyl)benzyl)phthalazin-1(2*H*)-one (20 mg, 0.055 mmol, 1.0 equiv.) was dissolved in DMF (0.5 ml). To this solution was added (*E*)-cyclooct-4-en-1-yl (2,5-dioxopyrrolidin-1-yl) carbonate (15 mg, 0.056 mmol, 1.02 equiv.) and the reaction mixture was stirred at room temperature for 18 h. It was then purified directly by preparative HPLC. This afforded (*E*)-cyclooct-4-en-1-yl 4-(2-fluoro-5-((4-oxo-3,4-dihydrophthalazin-1-yl)methyl)benzoyl)piperazine-1-carboxylate as a white solid (15 mg, 52% yield). $^1$H NMR (400 MHz, DMSO-$d_6$) δ 12.58 (s, 1H), 8.24 (d, *J* = 7.2 Hz, 1H), 7.94 (d, *J* = 8.0 Hz, 1H), 7.87 (dd, *J* = 7.5, 7.5 Hz, 1H), 7.81 (dd, *J* = 7.5, 7.5 Hz, 1H), 7.44-7.39 (m, 1H), 7.32 (d, *J* = 6.2 Hz, 1H), 7.21 (dd, *J* = 9.1, 9.1 Hz, 1H), 5.61-5.51 (m, 1H), 5.47-5.37 (m, 1H), 4.31 (s, 2H), 4.26-4.19 (m, 1H), 3.60-3.53 (m, 2H), 3.37-3.33 (m, 2H), 3.24-3.19 (m, 2H), 3.15-3.09 (m, 2H), 2.30-2.21 (m, 3H), 1.95-1.80 (m, 4H), 1.64-1.55 (m, 3H). LC-MS (ESI, m/z): $t_R$ = 2.62 min, 519.4 $(M+H)^+$. HRMS-ESI *m/z* calculated for $C_{29}H_{32}FN_4O_4$ 519.2402 $[M+H]^+$ found 519.2403

**(*E*)-cyclooct-4-en-1-yl(2-(5-(4-(2-fluoro-5-((4-oxo-3,4-dihydrophthalazin-1-yl)methyl)benzoyl)piperazin-1-yl)-5-oxopentanamido)ethyl)carbamate** (**3**)

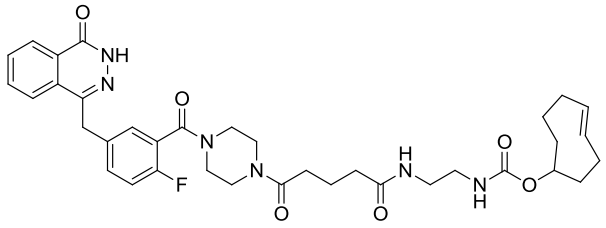

*N*-(2-aminoethyl)-5-(4-(2-fluoro-5-((4-oxo-3,4-dihydrophthalazin-1-yl)methyl)benzoyl)piperazin-1-yl)-5-oxopentanamide (15 mg, 0.029 mmol, 1.0 equiv.) was dissolved in DMF (0.2 ml). To this solution was added (*E*)-cyclooct-4-en-1-yl (2,5-dioxopyrrolidin-1-yl) carbonate (8 mg, 0.029 mmol, 1.0 equiv.). The reaction mixture was then stirred at room temperature for 2 h and then it was purified by preparative HPLC. This afforded (*E*)-cyclooct-4-en-1-yl (2-(5-(4-(2-fluoro-5-((4-oxo-3,4-dihydrophthalazin-1-yl)methyl)benzoyl) piperazin-1-yl)-5-oxopentanamido)ethyl) carbamate as a white solid (8 mg, 41% yield). $^1$H NMR (400 MHz, DMSO-$d_6$) δ 12.60 (s, 1H), 8.24 (d, *J* = 7.2, 1H), 7.95 (d, *J* = 7.4, 1H), 7.92 – 7.72 (m, 3H), 7.43 (s, 1H), 7.35 (s, 1H), 7.23 (dd, *J* = 7.9, 8.7, 1H), 6.97-6.91 (m, 1H), 5.60-5.49 (m, 1H), 5.46-5.37 (m, 1H), 4.31 (s, 2H), 4.20-4.14 (s, 1H), 3.64 – 3.47 (m, 8H), 3.05-2.94 (m, 4H), 2.67-2.62 (m, 2H), 2.33-2.28 (m, 2H) 2.27-2.20 (m, 3H), 2.10-2.03 (m, 2H), 1.94-1.82 (m, 3H), 1.74-1.52 (m, 4H). LC-MS (ESI, m/z): $t_R$ = 2.09 min, 675.4 $(M+H)^+$. HRMS-ESI *m/z* calculated for $C_{36}H_{44}FN_6O_6$ 675.3301 $[M+H]^+$ found 675.3297

**(*E*)-cyclooct-2-en-1-yl 4-(2-fluoro-5-((4-oxo-3,4-dihydrophthalazin-1-yl)methyl)benzoyl)piperazine-1-carboxylate** (**4**)

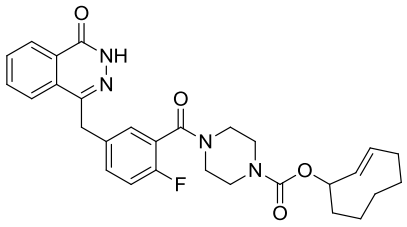

4-(4-fluoro-3-(piperazine-1-carbonyl)benzyl)phthalazin-1(2*H*)-one (20 mg, 0.055 mmol, 1.0 equiv.) was dissolved in DMF (0.5 ml). To this solution was added *E*)-cyclooct-2-enyl (4-nitrophenyl) carbonate (16 mg, 0.056 mmol, 1.02 equiv.) and the reaction mixture was stirred at room temperature for 2h. The reaction mixture was then purified by preparative HPLC to afford (*E*)-cyclooct-2-en-1-yl 4-(2-fluoro-5-((4-oxo-3,4-dihydrophthalazin-1-yl)methyl)benzoyl)piperazine-1-carboxylate as a white solid (19 mg, 67% yield). $^1$H NMR (400 MHz, DMSO-$d_6$) δ 12.59 (s, 1H), 8.24 (d, *J* = 7.6 Hz, 1H), 7.95 (d, *J* = 8.1 Hz, 1H), 7.90-7.79 (m, 2H), 7.46-7.40 (m, 1H), 7.34 (d, *J* = 6.4 Hz, 1H), 7.22 (dd, *J* = 9.3, 9.3 Hz, 1H), 5.76-5.69 (m, 1H), 5.60-5.50 (m, 1H) 5.08-4.96 (m, 1H), 4.31 (s, 2H), 3.65-3.52 (m, 4H), 3.29-3.22 (m, 2H), 3.19-3.12 (m, 2H), 2.17-2.01 (m, 2H), 1.99-1.84 (m, 2H), 1.83-1.66 (m, 2H), 1.59-1.33 (m, 2H), 0.97-0.72 (m, 2H). LC-MS (ESI, m/z): $t_R$ = 2.66 min, 519.4 $(M+H)^+$. HRMS-ESI *m/z* calculated for $C_{29}H_{32}FN_4O_4$ 519.2402 $[M+H]^+$ found 519.2400

**(*E*)-cyclooct-2-en-1-yl(2-(5-(4-(2-fluoro-5-((4-oxo-3,4-dihydrophthalazin-1-yl)methyl)benzoyl)piperazin-1-yl)-5-oxopentanamido)ethyl)carbamate** (**5**)

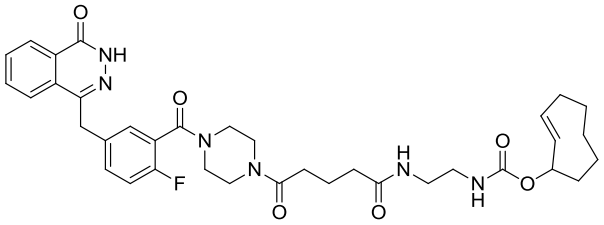

*N*-(2-aminoethyl)-5-(4-(2-fluoro-5-((4-oxo-3,4-dihydrophthalazin-1-yl)methyl)benzoyl)piperazin-1-yl)-5-oxopentanamide (15 mg, 0.029 mmol, 1.0 equiv.) was dissolved in DMF (0.2 ml). To this solution was added (*E*)-cyclooct-2-enyl (4-nitrophenyl) carbonate (8 mg, 0.029 mmol, 1.0 equiv.). The reaction mixture was then stirred at room temperature for 2 h and then it was purified by preparative HPLC. This afforded (*E*)-cyclooct-2-en-1-yl(2-(5-(4-(2-fluoro-5-((4-oxo-3,4-dihydrophthalazin-1-yl)methyl)benzoyl)piperazin-1-yl)-5-oxopentanamido)ethyl)carbamate as a white solid (10 mg, 51% yield). $^1$H NMR (400 MHz, DMSO-$d_6$) δ 12.59 (s, 1H), 8.25 (d, *J* = 8.1 Hz, 1H), 7.95 (d, *J* = 8.0 Hz, 1H), 7.92 – 7.68 (m, 3H), 7.42 (s, 1H), 7.37-7.32 (m, 1H), 7.22 (dd, *J* = 9.0, 9.0 Hz, 1H), 7.05 (s, 1H), 5.73-5.62 (m, 1H), 5.52-5.44 (m, 1H), 4.97-4.89 (m, 1H), 4.32 (s, 2H), 3.69-3.45 (m, 4H), 3.19 – 2.89 (m, 4H), 2.67-2.61 (m, 2H), 2.31-2.16 (m, 2H), 2.1-2.02 (s, 3H), 1.93-1.82 (m, 3H), 1.76-1.62 (m, 4H), 1.43-1.29 (m, 3H), 0.91-0.67 (m, 3H). LC-MS (ESI, m/z): $t_R$ = 2.12 min, 675.5 $(M+H)^+$. HRMS-ESI *m/z* calculated for $C_{36}H_{44}FN_6O_6$ 675.3301 $[M+H]^+$ found 675.3296

**(1*R*,8*S*,9*s*)-bicyclo[6.1.0]non-4-yn-9-ylmethyl 4-(2-fluoro-5-((4-oxo-3,4-dihydrophthalazin-1-yl)methyl)benzoyl)piperazine-1-carboxylate** (**6**)

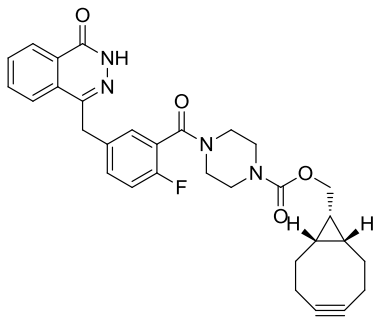

4-(4-fluoro-3-(piperazine-1-carbonyl)benzyl)phthalazin-1(2*H*)-one (20 mg, 0.055 mmol, 1.0 equiv.) was dissolved in DMF (0.5 ml). To this solution was added (1*R*,8*S*,9*s*)-bicyclo[6.1.0]non-4-yn-9-ylmethyl (2,5-

dioxopyrrolidin-1-yl)carbonate (16 mg, 0.056 mmol, 1.02 equiv.). The reaction mixture was then stirred at room temperature for 18 h. It was then purified by preparative HPLC to afford (1*R*,8*S*,9*s*)-bicyclo[6.1.0]non-4-yn-9-ylmethyl 4-(2-fluoro-5-((4-oxo-3,4-dihydrophthalazin-1-yl)methyl)benzoyl)piperazine-1-carboxylate as a white solid(3 mg, 10% yield). $^1$H NMR (400 MHz, Methanol-$d_4$) δ 8.37 (d, *J* = 7.2 Hz, 1H), 7.95 (d, *J* = 7.2 Hz, 1H), 7.87-7.83 (m, 2H), 7.51-7.46 (m, 1H), 7.39-7.35 (m, 1H), 7.16 (dd, 9.5, 9.5, 1H), 5.50 (s, 2H), 4.38 (s, 2H), 4.22 (d, *J* = 8.3 Hz, 2H), 3.76-3.71 (m, 2H), 3.61-3.54 (m, 2H), 2.94-2.89 (m, 2H), 2.31-2.14 (m, 6H), 1.69-1.55 (m, 2H), 1.44-1.28 (m, 2H), 1.00-0.97 (m, 1H). LC-MS (ESI, m/z): $t_R$ = 2.51 min, 543.4 $(M+H)^+$. HRMS-ESI *m/z* calculated for $C_{31}H_{32}FN_4O_4$ 543.2402 $[M+H]^+$ found 543.2400

**(1*R*,8*S*,9*s*)-bicyclo[6.1.0]non-4-ylmethyl (2-(5-(4-(2-fluoro-5-((4-oxo-3,4-dihydrophthalazin-1-yl)methyl) benzoyl) piperazin-1-yl)-5-oxopentanamido)ethyl)carbamate** (**7**)

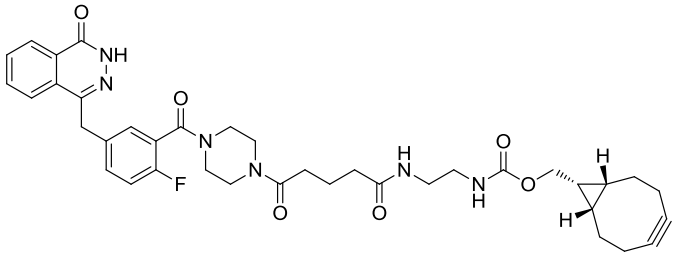

*N*-(2-aminoethyl)-5-(4-(2-fluoro-5-((4-oxo-3,4-dihydrophthalazin-1-yl)methyl)benzoyl)piperazin-1-yl)-5-oxopentanamide (15 mg, 0.029 mmol, 1.0 equiv.) was dissolved in DMF (0.2 ml). To this solution was added ((1*R*,8*S*,9*s*)-bicyclo[6.1.0]non-4-yn-9-ylmethyl (2,5-dioxopyrrolidin-1-yl)carbonate (8 mg, 0.029 mmol, 1.0 equiv.). The reaction mixture was then stirred at room temperature for 1 h and then it was purified by preparative HPLC. This afforded (*E*)-cyclooct-4-en-1-yl(2-(5-(4-(2-fluoro-5-((4-oxo-3,4-dihydrophthalazin-1-yl)methyl)benzoyl)piperazin-1-yl)-5-oxopentanamido)ethyl)carbamate as a white solid (5 mg, 25% yield). $^1$H NMR (400 MHz, DMSO-$d_6$) δ 12.59 (s, 1H), 8.24 (d, *J* = 7.3 Hz, 1H), 7.95 (d, *J* = 8.3 Hz, 1H), 7.91-7.78 (m, 3H), 7.42 (s, 1H), 7.35 (s, 1H), 7.22 (dd, *J* = 10.1, 7.4, 1H), 7.11-7.06 (m, 1H), 4.31 (s, 2H), 3.97-4.01 (m, 2H), 3.63-3.47 (m, 4H), 3.07-2.96 (m, 4H), 2.69-2.65 (m, 2H), 2.28-2.04 (m, 10H), 1.73-1.64 (m, 2H), 1.53-1.39 (m, 3H), 1.32-1.18 (m, 2H), 0.89-0.78 (m, 2H). LC-MS (ESI, m/z): $t_R$ = 2.04 min, 699.5 $(M+H)^+$. HRMS-ESI *m/z* calculated for $C_{38}H_{44}FN_6O_6$ 699.3301 $[M+H]^+$ found 699.3299

***N*-(3-azidopropyl)-5-(4-(2-fluoro-5-((4-oxo-3,4-dihydrophthalazin-1-yl)methyl)benzoyl)piperazin-1-yl)-5-oxopentanamide** (**8**)

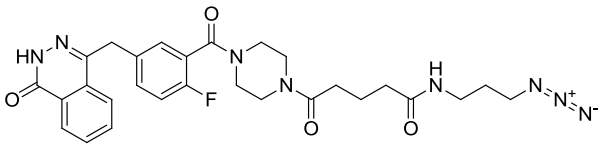

5-(4-(2-fluoro-5-((4-oxo-3,4-dihydrophthalazin-1-yl)methyl)benzoyl)piperazin-1-yl)-5-oxopentanoic acid (23 mg, 0.048 mmol, 1.0 equiv.) was dissolved in DMF (0.5 ml). To this solution was added 3-azidopropan-1-amine (5 mg, 0.052 mmol, 1.1 equiv) followed by Bromotripyrrolidinophosphonium hexafluorophosphate (24 mg, 0.052 mmol, 1.1 equiv.) and DIPEA (17 μl, 0.096 mmol, 2.0 equiv.) and the reaction mixture was stirred at room temperature for 3h. It was then purified directly by preparative HPLC to afford *N*-(3-azidopropyl)-5-(4-(2-fluoro-5-((4-oxo-3,4-dihydrophthalazin-1-yl)methyl)benzoyl)piperazin-1-yl)-5-oxopentanamide (22 mg, 82% yield) as a white solid. $^1$H NMR (400 MHz, DMSO-$d_6$) δ 12.61 (s, 1H), 8.27 (d, *J* = 7.6 Hz, 1H), 7.97(d, *J* = 8.0 Hz, 1H) 7.92-7.89 (m, 1H), 7.88-7.82 (m, 2H), 7.45 (s, 1H), 7.37 (s, 1H), 7.25(dd, *J* = 9.0, 9.0, 1H), 4.34 (s, 2H), 3.66-3.62 (m,

1H), 3.60-3.55 (m, 1H), 3.54-3.49 (m, 2H), 3.39 – 3.36 (m, 4H), 3.21-3.13 (m, 2H), 3.12-3.05 (m, 2H), 2.30 (dt, *J* = 27.3, 7.9 Hz, 2H), 2.15 – 2.05 (m, 2H), 1.75-1.69 (m, 2H), 1.66-1.59 (m, 2H). LC-MS (ESI, m/z): $t_R$ = 1.70 min, 563.3 $(M+H)^+$. HRMS-ESI *m/z* calculated for $C_{28}H_{32}FN_8O_4$ 563.2525 $[M+H]^+$ found 563.2521

**5-(4-(2-fluoro-5-((oxo-3,4-dihydrophthalazin-1-yl)methyl)benzoyl)piperazin-1-yl)-5-oxo-*N*-(2-propiolamidoethyl)pentanamide** (**9**)

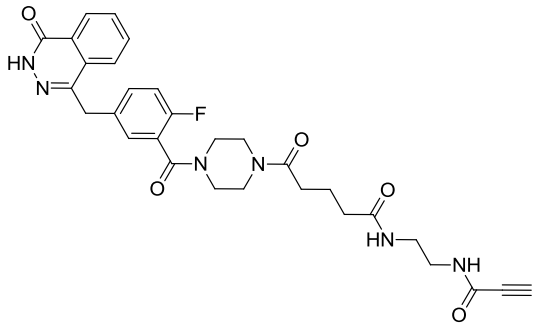

*N*-(2-aminoethyl)-5-(4-(2-fluoro-5-((4-oxo-3,4-dihydrophthalazin-1-yl)methyl)benzoyl)piperazin-1-yl)-5-oxopentanamide (20 mg, 0.038 mmol, 1.0 equiv.) was dissolved in DMF (0.5 ml). To this was added propiolic acid (2.5 μl, 0.042 mmol, 1.0 equiv.) followed by Bromotripyrrolidinophosphonium hexafluorophosphate (21 mg, 0.045 mmol, 1.2 equiv.) and triethylamine (11 μl, 0.077 mmol, 2.0 equiv.). The reaction mixture was then stirred at room temperature for 2h and then purified directly by preparative HPLC. This afforded 5-(4-(2-fluoro-5-((oxo-3,4-dihydrophthalazin-1-yl)methyl)benzoyl)piperazin-1-yl)-5-oxo-*N*-(2-propiolamidoethyl)pentanamide (9 mg, 41% yield) as a white solid. $^1$H NMR (400 MHz, DMSO-$d_6$) δ 12.58 (s, 1H), 8.67 (s, 1H), 8.27 (d, *J* = 7.6 Hz, 1H), 7.97 (d, *J* = 7.9 Hz, 1H), 7.92-7.88 (m, 1H), 7.88 – 7.78 (m, 2H), 7.54 – 7.43 (m, 1H), 7.37 (s, 1H), 7.24 (dd, *J* = 9.0, 9.0, 1H), 4.34 (s, 2H), 4.10 (d, *J* = 8.4 Hz, 1H), 3.64-3.52 (m, 4H), 3.41-3.36 (m, 3H) 3.20-3.09 (m, 5H), 2.34-2.26 (m, 2H), 2.12-2.08 (m, 2H), 1.74-1.69 (m, 2H). LC-MS (ESI, m/z): $t_R$ = 1.42 min, 575.3 $(M+H)^+$. HRMS-ESI *m/z* calculated for $C_{30}H_{32}FN_6O_5$ 575.2413 $[M+H]^+$ found 575.2408

**(*R*)-1-(3-(4-amino-3-(4-phenoxyphenyl)-1*H*-pyrazolo[3,4-*d*]pyrimidin-1-yl)piperidin-1-yl)prop-2-en-1-one** (**10**)

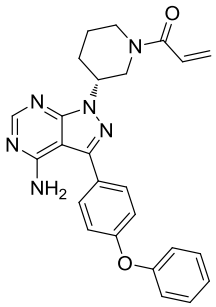

(*R*)-1-(3-(4-amino-3-(4-phenoxyphenyl)-1*H*-pyrazolo[3,4-*d*]pyrimidin-1-yl)piperidin-1-yl)prop-2-en-1-one was purchased from Selleckchem and used as received.

**(*R*,*E*)-1-(3-(4-amino-3-(4-phenoxyphenyl)-1H-pyrazolo[3,4-d]pyrimidin-1-yl)piperidin-1-yl)-4-(4-(2-aminoethyl)piperazin-1-yl)but-2-en-1-one 2,2,2-trifluoroacetate salt.**

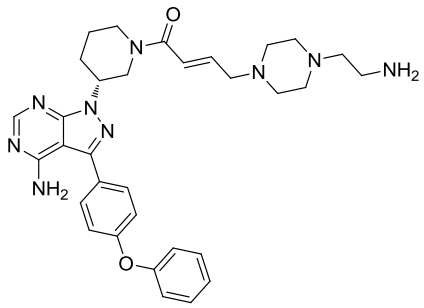

(*R*,*E*)-1-(3-(4-amino-3-(4-phenoxyphenyl)-1*H*-pyrazolo[3,4-d]pyrimidin-1-yl)piperidin-1-yl)-4-(4-(2-aminoethyl)piperazin-1-yl)but-2-en-1-one 2,2,2-trifluoroacetate salt was prepared as described.[14]

**(*R*,*E*)-*N*-(2-(4-(4-(3-(4-amino-3-(4-phenoxyphenyl)-1*H*-pyrazolo[3,4-d]pyrimidin-1-yl)piperidin-1-yl)-4-oxobut-2-en-1-yl)piperazin-1-yl)ethyl)-5-azidopentanamide** (**11**)

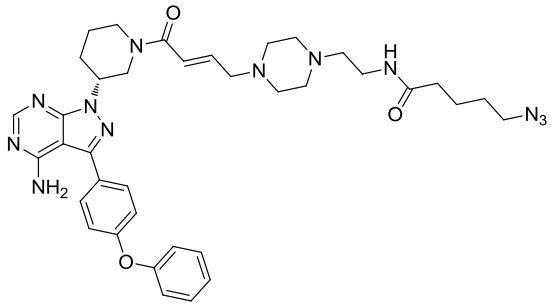

(*R*,*E*)-1-(3-(4-amino-3-(4-phenoxyphenyl)-1*H*-pyrazolo[3,4-d]pyrimidin-1-yl)piperidin-1-yl)-4-(4-(2-aminoethyl)piperazin-1-yl)but-2-en-1-one 2,2,2-trifluoroacetate salt (13.5 mg, 0.020 mmol, 1 equiv.) was dissolved in DMF (0.4 ml). To this solution was added 2,5-dioxopyrrolidin-1-yl 5-azidopentanoate (7.0 mg, 0.030 mmol, 1.5 equiv.) followed by triethylamine (5.9 mg, 0.058 mmol, 3 equiv.). The reaction was stirred at room temperature for 1 hour and then purified by preparative HPLC. This afforded (*R*,*E*)-*N*-(2-(4-(4-(3-(4-amino-3-(4-phenoxyphenyl)-1*H*-pyrazolo[3,4-d]pyrimidin-1-yl)piperidin-1-yl)-4-oxobut-2-en-1-yl)piperazin-1-yl)ethyl)-5-azidopentanamide (yield: 5.5 mg, 0.008 mmol, 40 %). $^1$H NMR (400 MHz, Chloroform-*d*) δ 8.37 (d, *J* = 9.5 Hz, 1H), 7.66 (d, *J* = 8.3 Hz, 2H), 7.42 (dd, *J* = 7.8, 7.8 Hz, 2H), 7.23 – 7.17 (m, 3H), 7.11 (d, *J* = 8, 2H), 6.88-6.73 (m, 1H), 6.52-6.39 (m, 1H), 5.80 (s, 2H), 4.88 (s, 2H),4.53 (d, *J* = 12.0, 1H), 4.15 (d, *J* = 13.2 Hz, 1H), 4.03 (d, J = 12, 1H), 3.86-3.80 (m, 1H), 3.54 (s, 2H), 3.44-3.08 (m, 5H), 3.02-2.61 (m, 10H), 2.50-2.34 (m, 1H), 2.30-2.23 (m, 2H), 2.10-1.99 (m, 1H), 1.77-1.71 (m, 2H) and 1.68-1.59 (m, 2H). LC-MS (ESI, m/z): $t_R$ = 1.86 min, 706.0 $(M+H)^+$. HRMS-ESI *m/z* calculated for $C_{37}H_{47}N_{12}O_3$ 707.3889 $[M+H]^+$ found 707.3882

**(*E*)-cyclooct-4-en-1-yl(2-(4-((*E*)-4-((*R*)-3-(4-amino-3-(4-phenoxyphenyl)-1*H*-pyrazolo[3,4-d]pyrimidin-1-yl)piperidin-1-yl)-4-oxobut-2-en-1-yl)piperazin-1-yl)ethyl)carbamate** (**12**)

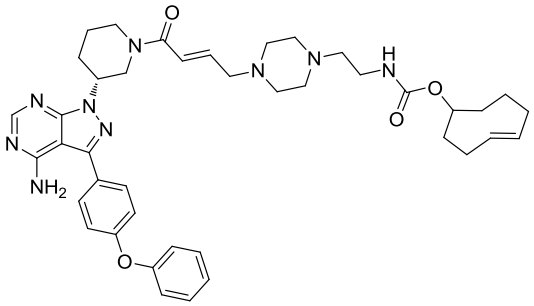

(*R*,*E*)-1-(3-(4-amino-3-(4-phenoxyphenyl)-1*H*-pyrazolo[3,4-d]pyrimidin-1-yl)piperidin-1-yl)-4-(4-(2-aminoethyl)piperazin-1-yl)but-2-en-1-one 2,2,2-trifluoroacetate salt (20.0 mg, 0.029 mmol, 1 equiv.) was dissolved in DMF (0.5 ml). To this solution was added (*E*)-cyclooct-4-en-1-yl (2,5-dioxopyrrolidin-1-yl) carbonate (8.5 mg, 0.032 mmol, 1.1 equiv.) followed by triethylamine (8.7 mg, 0.086 mmol, 3 equiv.). The reaction was stirred at room temperature for 2.5 hours and then purified by preparative HPLC. This afforded (*E*)-cyclooct-4-en-1-yl (2-(4-((*E*)-4-((*R*)-3-(4-amino-3-(4-phenoxyphenyl)-1*H*-pyrazolo[3,4-d]pyrimidin-1-yl)piperidin-1-yl)-4-oxobut-2-en-1-yl)piperazin-1-yl)ethyl)carbamate (yield: 12.1 mg, 0.016 mmol, 57 %). $^1$H NMR (400 MHz, DMSO-$d_6$) δ 8.25 (s, 1H), 8.15 (s, 1H), 7.65 (d, *J* = 8.1 Hz, 2H), 7.49–7.38 (m, 2H), 7.24–7.09 (m, 5H), 6.86–6.73 (m, 1H), 6.71 – 6.57 (m, 1H), 6.51–6.41 (m, 1H), 5.69–5.35 (m, 2H), 4.26–4.14 (m, 1H), 4.15–3.96 (m, 5H), 3.14–2.87 (m, 4H), 2.45–2.06 (m, 14H), 2.03 – 1.77 (m, 5H), 1.69–1.42 (m, 5H). LC-MS (ESI, m/z): $t_R$ = 2.13 min, 732.6 $(M-H)^-$. HRMS-ESI *m/z* calculated for $C_{41}H_{52}N_9O_4$ 734.4137 $[M+H]^+$ found 734.4129

**_N_-(4-(1,2,4,5-tetrazin-3-yl)benzyl)-1-(5-((3a*S*,4*S*,6a*S*)-2-oxohexahydro-1*H*-thieno[3,4-d]imidazol-4-yl)pentanamido)-3,6,9,12-tetraoxapentadecan-15-amide** (**13**)

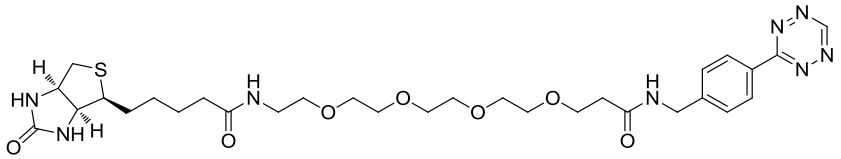

2,5-dioxopyrrolidin-1-yl 17-oxo-21-((3a*S*,4*S*,6a*R*)-2-oxohexahydro-1*H*-thieno[3,4-d]imidazol-4-yl)-4,7,10,13-tetraoxa-16-azahenicosan-1-oate (10 mg, 0.017 mmol, 1.0 equiv.) was dissolved in DMF (0.5 ml) and to this was added the hydrochloric acid salt of (4-(1,2,4,5-tetrazin-3-yl)phenyl)methanamine (3 mg, 0.017 mmol, 1.0 equiv.) and DIPEA (4 μl, 0.026, 1.5 equiv.). The reaction mixture was then stirred at room temperature for 2 h and purified directly by preparative HPLC. This afforded *N*-(4-(1,2,4,5-tetrazin-3-yl)benzyl)-1-(5-((3a*S*,4*S*,6a*S*)-2-oxohexahydro-1*H*-thieno[3,4-d]imidazol-4-yl)pentanamido)-3,6,9,12-tetraoxapentadecan-15-amide (11 mg, 98% yield) as a pink oil. $^1$H NMR (400 MHz, DMSO-$d_6$) δ 10.57 (s, 1H), 8.52 (s, 1H), 8.44 (d, *J* = 8.3 Hz, 2H), 7.82 (s, 1H), 7.53 (d, *J* = 8.3 Hz, 2H), 6.41 (s, 1H), 6.35 (s, 1H), 4.40 (d, *J* = 6.0 Hz, 2H), 4.27 (d, *J* = 6.5 Hz, 1H), 4.12-4.08 (m, 1H), 3.65 (t, *J* = 6.3 Hz, 2H), 3.56 – 3.44 (m, 11H), 3.22 – 3.01 (m, 4H), 2.80 (dd, *J* = 12.4, 4.9 Hz, 2H), 2.44-2.40 (m, 4H), 2.04 (t, *J* = 7.4 Hz, 2H), 1.52-1.41 (m, 3H), 1.32-1.21 (m, 2H). LC-MS (ESI, m/z): $t_R$ = 1.53 min, 683.3 $(M+Na)^+$. HRMS-ESI *m/z* calculated for $C_{30}H_{45}N_8O_7S$ 661.3126 $[M+H]^+$ found 661.3122

**_N_-4-(6-methyl-1,2,4,5-tetrazin-3-yl)benzyl)-1-(5-((3a*S*,4*S*,6a*S*)-2-oxohexahydro-1*H*-thieno[3,4-d]imidazol-4-yl)pentanamido)-3,6,9,12-tetraoxapentadecan-15-amide** (**14**)

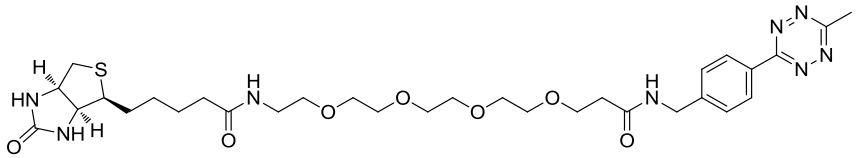

2,5-dioxopyrrolidin-1-yl 17-oxo-21-((3a*S*,4*S*,6a*R*)-2-oxohexahydro-1*H*-thieno[3,4-d]imidazol-4-yl)-4,7,10,13-tetraoxa-16-azahenicosan-1-oate (10 mg, 0.017 mmol, 1.0 equiv.) was dissolved in DMF (0.5 ml) and to this was added the hydrochloric acid salt of (4-(6-methyl-1,2,4,5-tetrazin-3-yl)phenyl)methanamine (3 mg, 0.017 mmol, 1.0 equiv.) and DIPEA (4 µl, 0.026 mmol, 1.5 equiv.). The reaction mixture was then stirred at room temperature for 2 h and purified directly by preparative HPLC. This afforded *N*-4-(6-methyl-1,2,4,5-tetrazin-3-yl)benzyl)-1-(5-((3a*S*,4*S*,6a*S*)-2-oxohexahydro-1*H*-thieno[3,4-d]imidazol-4-yl)pentanamido)-3,6,9,12-tetraoxapentadecan-15-amide (9 mg, 79% yield) as a pink oil. $^1$H NMR (400 MHz, DMSO-$d_6$) δ 8.51 (s, 1H), 8.40 (d, *J* = 8.1 Hz, 2H), 7.82 (s, 1H), 7.51 (d, *J* = 8.1 Hz, 2H), 6.41 (s, 1H), 6.34 (s, 1H), 4.39 (d, *J* = 6.0 Hz, 2H), 4.31-4.26 (m, 1H), 4.11 (s, 1H), 3.65 (t, *J* = 6.3 Hz, 3H), 3.52 – 3.43 (m, 13H), 3.15 (d, *J* = 5.8 Hz, 1H), 3.09-3.04 (m, 1H), 2.98 (s, 3H), 2.89 – 2.73 (m, 2H), 2.42 (t, *J* = 6.3 Hz, 2H), 2.03 (t, *J* = 7.4 Hz, 2H), 1.63-1.53 (m, 2H), 1.49-1.40 (m, 3H), 1.30-1.24 (m, 2H). LC-MS (ESI, m/z): $t_R$ = 1.63 min, 697.3 $(M+Na)^+$. HRMS-ESI *m/z* calculated for $C_{31}H_{47}N_8O_7S$ 675.3282 $[M+H]^+$ found 675.3277

**_N_-(2-(2-(2-(2-azidoethoxy)ethoxy)ethoxy)ethyl)-5-((3a*S*,4*S*,6a*R*)-2-oxohexahydro-1*H*-thieno[3,4-*d*]imidazol-4-ylpentanamide** (**15**)

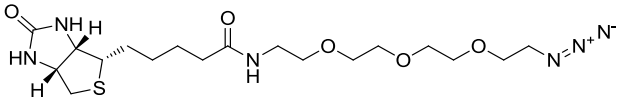

N-(2-(2-(2-(2-azidoethoxy)ethoxy)ethoxy)ethyl)-5-((3aS,4S,6aR)-2-oxohexahydro-1H-thieno[3,4-d]imidazol-4-ylpentanamide was purchased from TCI Europe N.V. and used as received.

**(*E*)-cyclooct-2-en-1-yl(13-oxo-17-(2-oxohexahydro-1*H*-thieno[3,4-*d*]imidazol-4-yl)-3,6,9-trioxa-12-azaheptadecyl)carbamate** (**16**)

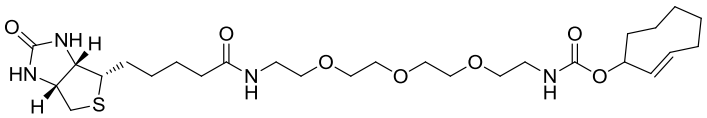

*N*-(2-(2-(2-(2-aminoethoxy)ethoxy)ethoxy)ethyl)-5-(2-oxohexahydro-1*H*-thieno[3,4-*d*]imidazol-4-yl)pentanamide (10 mg, 0.024 mmol, 1.0 equiv.) was dissolved in DMF (0.3 ml) and to this was added (*E*)-cyclooct-2-en-1-yl (4-nitrophenyl) carbonate (7 mg, 0.024 mmol, 1.0 equiv.). The reaction mixture was stirred at room temperature for 2 h and then purified by preparative HPLC. This afforded (*E*)-cyclooct-2-en-1-yl (13-oxo-17-(2-oxohexahydro-1*H*-thieno[3,4-*d*]imidazol-4-yl)-3,6,9-trioxa-12-azaheptadecyl)carbamate (4 mg, 29% yield) as a yellow oil. $^1$H NMR (400 MHz, DMSO-$d_6$) δ 7.82 (t, *J* = 4.4, 1H), 7.06 (t, *J* = 4.9, 1H), 6.41 (s, 1H), 6.35 (s, 1H), 5.74-5.65 (m, 1H), 5.50 (dd, *J* = 16.3, 9.6 Hz, 1H), 5.00-4.91 (m, 1H), 4.35 – 4.24 (m, 1H), 4.13-4.08 (m, 1H), 3.49-3.46 (m, 8H), 3.38-3.35 (m, 4H), 3.15 (dd, *J* = 10.7, 4.6 Hz, 2H), 3.10-3.06 (m, 3H), 2.80 (dd, *J* = 12.4, 5.1 Hz, 1H), 2.56 (d, *J* = 12.7 Hz, 2H), 2.32-2.29 (m, 1H), 2.11-2.02 (m, 3H), 1.97 – 1.86 (m, 2H), 1.80-1.68 (m, 2H), 1.61-1.39 (m, 5H), 1.37 – 1.20 (m, 2H), 0.92 – 0.71 (m, 2H). LC-MS (ESI, m/z): $t_R$ = 2.04 min, 571.3 $(M+H)^+$. HRMS-ESI *m/z* calculated for $C_{27}H_{46}N_4O_7S$ 571.3160 $[M+H]^+$ found 571.3154

**(1*R*,8*S*,9*s*)-bicyclo[6.1.0]non-4-yn-9-ylmethyl(13-oxo-17-((3a*S*,4*S*,6a*R*)-2-oxohexahydro-1*H*-thieno[3,4-*d*]imidazol-4-yl)-3,6,9-trioxa-12-azaheptadecyl)carbamate** (**17**)

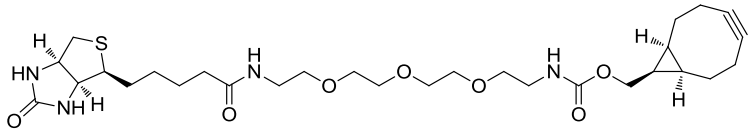

*N*-(2-(2-(2-(2-aminoethoxy)ethoxy)ethoxy)ethyl)-5-(2-oxohexahydro-1*H*-thieno[3,4-*d*]imidazol-4-yl)pentanamide (10 mg, 0.024 mmol, 1.0 equiv.) was dissolved in DMF (0.3 ml) and to this was added (1*R*,8*S*,9*S*)-bicyclo[6.1.0]non-4-yn-9-ylmethyl (2,5-dioxopyrrolidin-1-yl) carbonate (7 mg, 0.024 mmol, 1.0 equiv.). The reaction mixture was then stirred at room temperature for 2 h and purified directly by preparative HPLC. This afforded (1*R*,8*S*,9*s*)-bicyclo[6.1.0]non-4-yn-9-ylmethyl (13-oxo-17-((3a*S*,4*S*,6a*R*)-2-oxohexahydro-1*H*-thieno[3,4-*d*]imidazol-4-yl)-3,6,9-trioxa-12-azaheptadecyl)carbamate (8 mg, 56% yield) as a yellow oil. $^1$H NMR (400 MHz, DMSO-$d_6$) δ 7.28 (t, *J* = 5.2, 1H) 7.09 (t, *J* = 6.2, 1H), 6.41 (s, 1H), 6.34 (s, 1H), 4.31-4.26 (m, 1H), 4.12-4.08 (m, 1H), 4.01 (d, *J* = 8.0 Hz, 2H), 3.49-3.47 (m, 9H), 3.38-3.35 (m, 7H), 3.16 (dd, *J* = 11.5, 5.9 Hz, 1H), 3.13 – 3.02 (m, 2H), 2.79(dd, *J* = 12.5, 5.2, 1H), 2.66-2.64 m, 1H), 2.62 – 2.50 (m, 4H), 2.21-2.10 (m, 4H), 2.04 (t, *J* = 7.4 Hz, 1H), 1.63-1.40 (m, 4H), 1.41 – 1.17 (m, 2H), 0.84 (t, *J* = 10.0 Hz, 2H). LC-MS (ESI, m/z): $t^R$ = 1.94 min, 595.3 $(M+H)^+$. HRMS-ESI *m/z* calculated for $C_{29}H_{47}N_4O_7S$ 595.3160 $[M+H]^+$ found 595.3153

**5-((3a*S*,4*S*,6a*R*)-2-oxohexahydro-1*H*-thieno[3,4-*d*]imidazol-4-yl)-*N*-(3,6,9,12-tetraoxapentadec-14-yn-1-yl)pentanamide** (**18**)

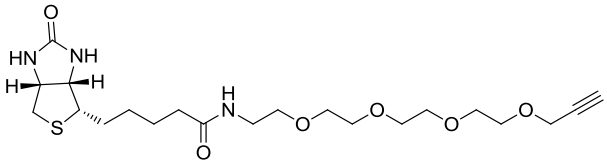

5-((3aS,4S,6aR)-2-oxohexahydro-1H-thieno[3,4-d]imidazol-4-yl)-N-(3,6,9,12-tetraoxapentadec-14-yn-1-yl)pentanamide was purchased form Polypeptide and used as received.

***N*-benzyl-1-(5-((3a*S*,4*S*,6a*R*)-2-oxohexahydro-1*H*-thieno[3,4-*d*]imidazol-4-yl)pentanamido)-3,6,9,12-tetraoxapentadecan-15-amide** (**19**)

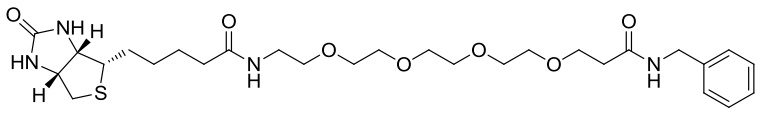

2,5-dioxopyrrolidin-1-yl 17-oxo-21-((3a*S*,4*S*,6a*R*)-2-oxohexahydro-1*H*-thieno[3,4-d]imidazol-4-yl)-4,7,10,13-tetraoxa-16-azahenicosan-1-oate (20 mg, 0.033 mmol, 1 equiv.) was dissolved in DMF (0.3 ml) and to this was added benzyl amine (4 mg, 0.037 mmol, 1.1 equiv.). The reaction mixture was then stirred at room temperature for 2h and then purified directly by preparative HPLC. This afforded N-benzyl-1-(5-((3aS,4S,6aR)-2-oxohexahydro-1H-thieno[3,4-d]imidazol-4-yl)pentanamido)-3,6,9,12-tetraoxapentadecan-15-amide (6 mg, 31% yield) as a colourless oil. $^1$H NMR (400 MHz, DMSO-$d_6$) δ 8.36 (t, *J* = 6.0 Hz, 1H), 7.84 (t, *J* = 5.7 Hz, 1H), 7.34 –

7.30 (m, 2H), 7.27-7.21 (m, 3H), 6.43 (s, 1H), 6.37 (s, 1H), 4.32-4.27 (m, 3H), 4.15-4.11 (m, 1H), 3.64 (t, *J* = 6.4 Hz, 2H), 3.51-3.49 (m, 10H), 3.39 (t, *J* = 5.9 Hz, 2H), 3.35 (s, 2H), 3.21 – 3.16 (m, 2H), 3.12-3.07 (m, 1H), 2.82 (dd, *J* = 12.4, 5.1 Hz, 1H), 2.58 (d, *J* = 12.4 Hz, 1H), 2.39 (t, *J* = 6.4 Hz, 2H), 2.07 (t, *J* = 7.4 Hz, 2H), 1.65 – 1.55 (m, 1H), 1.55-1.40 (m, 3H), 1.34-1.24 (m, 2H). LC-MS (ESI, m/z): $t_R$ = 1.53 min, 581.3 $(M+H)^+$. HRMS-ESI *m/z* calculated for $C_{28}H_{45}N_4O_7S$ 581.3004 $[M+H]^+$ found 581.2998

***N*-cyclooctyl-1-(5-((3a*S*,4*S*,6a*R*)-2-oxohexahydro-1*H*-thieno[3,4-d]imidazol-4-yl)pentanamido)3,6,9,12-tetraoxapentadecan-15-amide** (**20**)

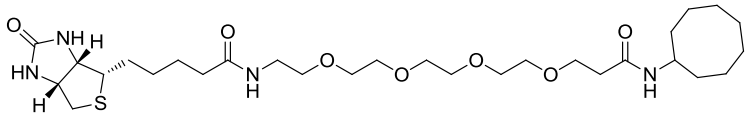

2,5-Dioxopyrrolidin-1-yl 17-oxo-21-((3a*S*,4*S*,6a*R*)-2-oxohexahydro-1*H*-thieno[3,4-d]imidazol-4-yl)-4,7,10,13-tetraoxa-16-azahenicosan-1-oate (20 mg, 0.034 mmol, 1.0 equiv.) was dissolved in DMF (0.3 ml) and to this was added cyclooctanamine (5 ml, 0.037 mmol, 1.1 equiv.). The reaction mixture was then stirred for 2 h at room temperature and purified directly by preparative HPLC. This afforded *N*-cyclooctyl-1-(5-((3a*S*,4*S*,6a*R*)-2-oxohexahydro-1*H*-thieno[3,4-*d*]imidazol-4-yl)pentanamido)3,6,9,12-tetraoxapentadecan-15-amide (7 mg, 34% yield) as a yellow oil. $^1$H NMR (400 MHz, DMSO-$d_6$) δ 7.85 (t, *J* = 5.7 Hz, 1H), 7.72 (d, *J* = 7.9 Hz, 1H), 6.43 (s, 1H), 6.36 (s, 1H), 4.32-4.29 (m, 1H), 4.15-4.11 (m, 1H), 3.81 – 3.69 (m, 1H), 3.58 (t, *J* = 6.5 Hz, 2H), 3.49 – 3.44 (m, 9H), 3.41-3.31 (m, 6H), 3.23 – 3.16 (m, 2H), 3.12-3.07 (m, 1H), 2.82 (dd, *J* = 12.4, 5.1 Hz, 1H), 2.58 (d, *J* = 12.4 Hz, 1H), 2.27 (t, *J* = 6.5 Hz, 2H), 2.07 (t, *J* = 7.4 Hz, 2H), 1.68-1.58 (m, 5H), 1.53 – 1.40 (m, 12H), 1.38 – 1.23 (m, 2H). LC-MS (ESI, m/z): $t_R$ = 1.89 min, 601.4 $(M+H)^+$. HRMS-ESI *m/z* calculated for $C_{29}H_{53}N_4O_7S$ 601.3630 $[M+H]^+$ found 601.3624

**8-fluoro-2-(4-((methylamino)methyl)phenyl)-4,5-dihydro-1*H*-azapin[5,4,3-*cd*]indol-6[3*H*)-one** (**21**)

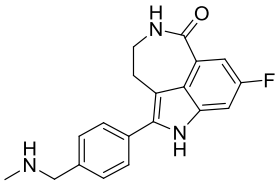

8-fluoro-2-(4-((methylamino)methyl)phenyl)-4,5-dihydro-1H-azapin[5,4,3-cd]indol-6[3H)-one was purchased fromSelleckchem and used as received.

**2-(dimethylamino)-*N*-)6-oxo-5,6-dihydrophenanthridin-2-yl)acetamide** (**22**)

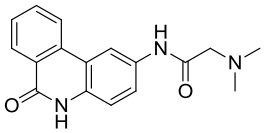

2-(dimethylamino)-N-)6-oxo-5,6-dihydrophenanthridin-2-yl)acetamide was purchased from Selleckchem as used as received.

**Table S1.** All compounds used in the study

| Compound Number | Structure |
|---|---|
| **1** (Olaparib) | 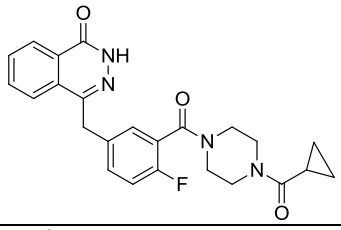 |
| **2** | 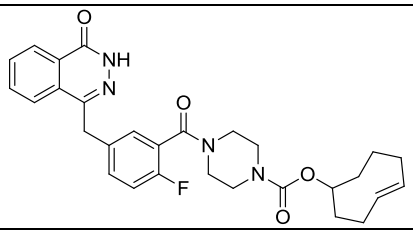 |
| **3** | 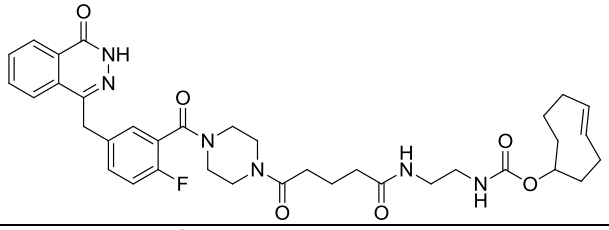 |
| **4** | 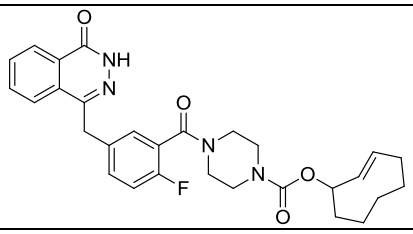 |
| **5** | 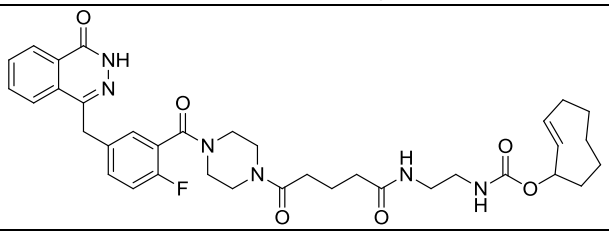 |
| **6** | 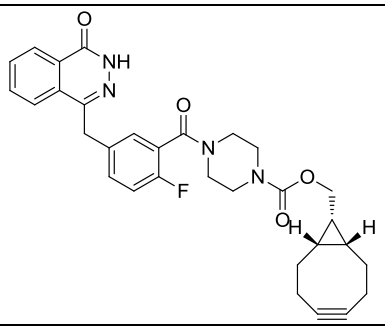 |
| **7** | 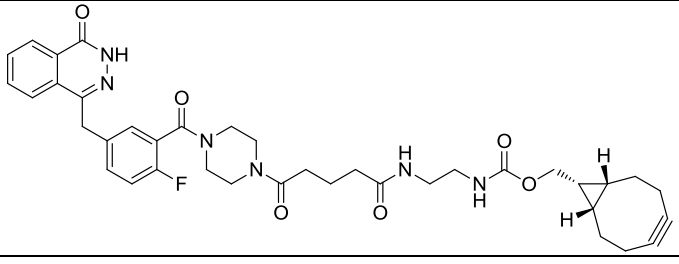 |

| | |
|---|---|
| **8** | 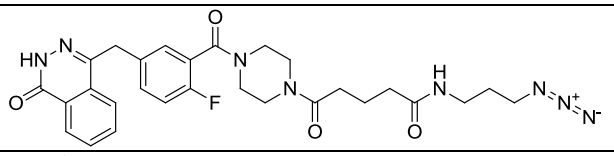 |
| **9** | 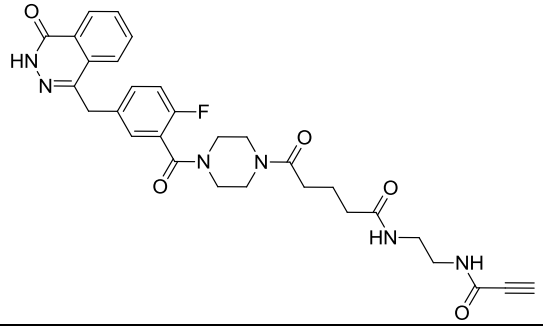 |
| **10** (Ibrutinib) | 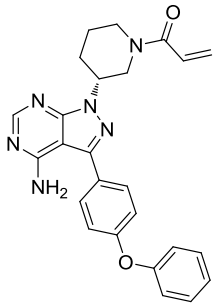 |
| **11** | 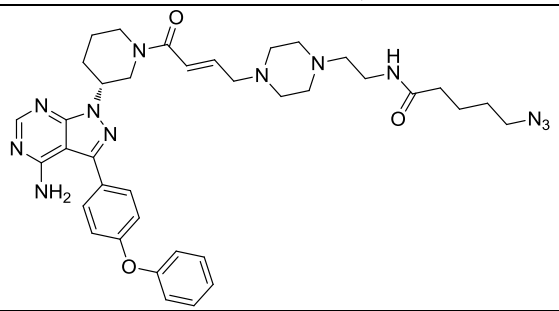 |
| **12** | 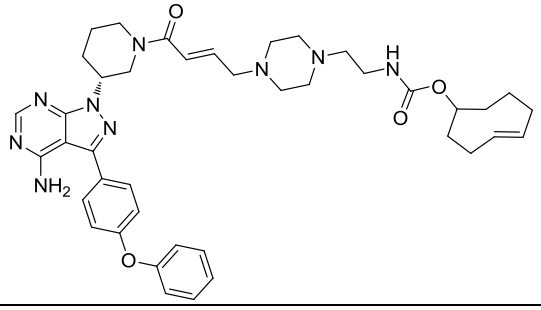 |
| **13** | 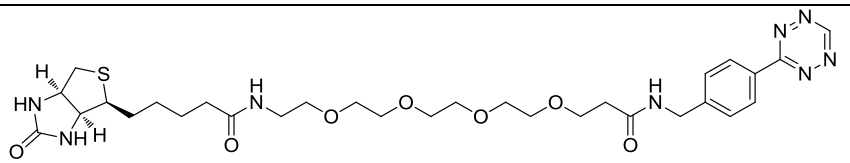 |
| **14** | 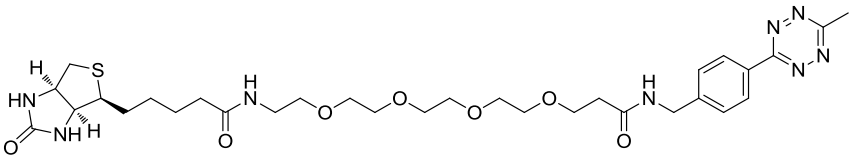 |
| **15** | 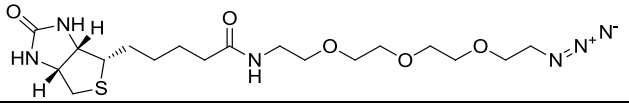 |

| | |
|---|---|
| **16** | 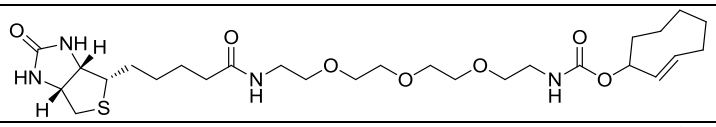 |
| **17** | 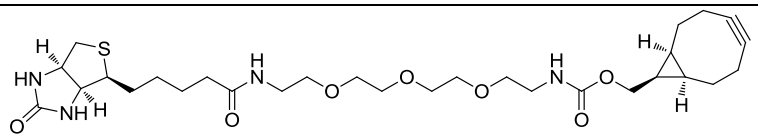 |
| **18** | 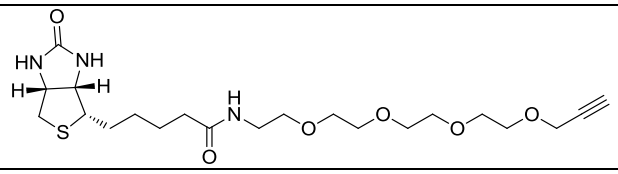 |
| **19** | 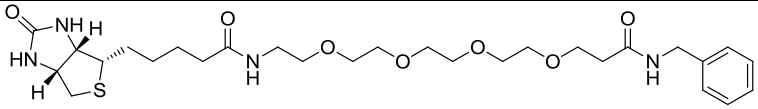 |
| **20** | 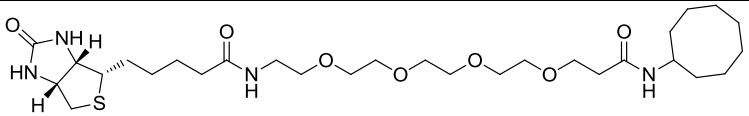 |
| **21** (Rucaparib) | 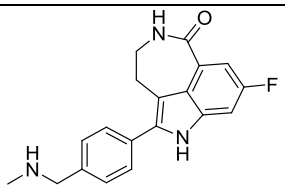 |
| **22** (PJ34) | 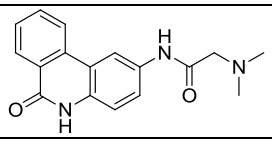 |

**References**

(1) Bantscheff, M., Eberhard, D., Abraham, Y., Bastuck, S., Boesche, M., Hobson, S., Mathieson, T., Perrin, J., Raida, M., Rau, C., Reader, V., Sweetman, G., Bauer, A., Bouwmeester, T., Hopf, C., Kruse, U., Neubauer, G., Ramsden, N., Rick, J., Kuster, B., and Drewes, G. (2007) Quantitative chemical proteomics reveals mechanisms of action of clinical ABL kinase inhibitors. *Nat. Biotechnol. 25*, 1035–1044.
(2) Speers, A. E., and Cravatt, B. F. (2009) Activity-Based Protein Profiling (ABPP) and Click Chemistry (CC)–ABPP by MudPIT Mass Spectrometry, in *Current Protocols in Chemical Biology*. John Wiley & Sons, Inc.
(3) Werner, T., Becher, I., Sweetman, G., Doce, C., Savitski, M. M., and Bantscheff, M. (2012) High-Resolution Enabled TMT 8-plexing. *Anal. Chem. 84*, 7188–7194.
(4) Werner, T., Sweetman, G., Savitski, M. F., Mathieson, T., Bantscheff, M., and Savitski, M. M. (2014) Ion Coalescence of Neutron Encoded TMT 10-Plex Reporter Ions. *Anal. Chem. 86*, 3594–3601.
(5) Franken, H., Mathieson, T., Childs, D., Sweetman, G. M. A., Werner, T., Tögel, I., Doce, C., Gade, S., Bantscheff, M., Drewes, G., Reinhard, F. B. M., Huber, W., and Savitski, M. M. (2015) Thermal proteome profiling for unbiased identification of direct and indirect drug targets using multiplexed quantitative mass spectrometry. *Nat. Protoc. 10*, 1567–1593.
(6) Savitski, M. M., Sweetman, G., Askenazi, M., Marto, J. A., Lang, M., Zinn, N., and Bantscheff, M. (2011) Delayed Fragmentation and Optimized Isolation Width Settings for Improvement of Protein Identification and Accuracy of Isobaric Mass Tag Quantification on Orbitrap-Type Mass Spectrometers. *Anal. Chem. 83*, 8959–8967.
(7) Savitski, M. M., Fischer, F., Mathieson, T., Sweetman, G., Lang, M., and Bantscheff, M. (2010) Targeted data acquisition for improved reproducibility and robustness of proteomic mass spectrometry assays. *J. Am. Soc. Mass Spectrom. 21*, 1668–1679.
(8) Savitski, M. M., Mathieson, T., Zinn, N., Sweetman, G., Doce, C., Becher, I., Pachl, F., Kuster, B., and Bantscheff, M. (2013) Measuring and Managing Ratio Compression for Accurate iTRAQ/TMT Quantification. *J. Proteome Res. 12*, 3586–3598.
(9) Silva, J. C., Gorenstein, M. V., Li, G.-Z., Vissers, J. P. C., and Geromanos, S. J. (2006) Absolute Quantification of Proteins by LCMSE A Virtue of Parallel ms Acquisition. *Mol. Cell. Proteomics 5*, 144–156.
(10) Becher, I., Savitski, M. M., Savitski, M. F., Hopf, C., Bantscheff, M., and Drewes, G. (2013) Affinity Profiling of the Cellular Kinome for the Nucleotide Cofactors ATP, ADP, and GTP. *ACS Chem. Biol. 8*, 599–607.
(11) Kim, E., Yang, K. S., Giedt, R. J., and Weissleder, R. (2014) Red Si–rhodamine drug conjugates enable imaging in GFP cells. *Chem. Commun. 50*, 4504–4507.
(12) Reiner, T., Earley, S., Turetsky, A., and Weissleder, R. (2010) Bioorthogonal Small-Molecule Ligands for PARP1 Imaging in Living Cells. *ChemBioChem 11*, 2374–2377.
(13) Menear, K. A., Adcock, C., Boulter, R., Cockcroft, X., Copsey, L., Cranston, A., Dillon, K. J., Drzewiecki, J., Garman, S., Gomez, S., Javaid, H., Kerrigan, F., Knights, C., Lau, A., Loh, V. M., Matthews, I. T. W., Moore, S., O'Connor, M. J., Smith, G. C. M., and Martin, N. M. B. (2008) 4-[3-(4-Cyclopropanecarbonylpiperazine-1-carbonyl)-4-fluorobenzyl]-2H-phthalazin-1-one: A Novel Bioavailable Inhibitor of Poly(ADP-ribose) Polymerase-1. *J. Med. Chem. 51*, 6581–6591.
(14) Liu, N., Hoogendoorn, S., Kar, B. van de, Kaptein, A., Barf, T., Driessen, C., Filippov, D. V., Marel, G. A. van der, Stelt, M. van der, and Overkleeft, H. S. (2015) Direct and two-step bioorthogonal probes for Bruton's tyrosine kinase based on ibrutinib: a comparative study. *Org. Biomol. Chem. 13*, 5147–5157.